

Sox2 and Lef-1 interact with Pitx2 to regulate incisor development and stem cell renewal

Zhao Sun^{1,*}, Wenjie Yu^{1,*}, Maria Sanz Navarro², Mason Sweat¹, Steven Eliason¹, Thad Sharp¹, Huan Liu^{1,3}, Kerstin Seidel⁴, Li Zhang³, Myriam Moreno¹, Thomas Lynch¹, Nathan E. Holton⁵, Laura Rogers¹, Traci Neff¹, Michael J. Goodheart⁶, Frederic Michon², Ophir D. Klein⁴, Yang Chai⁷, Adam Dupuy¹, John F. Engelhardt¹, Zhi Chen³ and Brad A. Amendt^{1,5,‡}

ABSTRACT

Sox2 marks dental epithelial stem cells (DESCs) in both mammals and reptiles, and in this article we demonstrate several Sox2 transcriptional mechanisms that regulate dental stem cell fate and incisor growth. Conditional Sox2 deletion in the oral and dental epithelium results in severe craniofacial defects, including impaired dental stem cell proliferation, arrested incisor development and abnormal molar development. The murine incisor develops initially but is absorbed independently of apoptosis owing to a lack of progenitor cell proliferation and differentiation. Tamoxifen-induced inactivation of Sox2 demonstrates the requirement of Sox2 for maintenance of the DESCs in adult mice. Conditional overexpression of Lef-1 in mice increases DESC proliferation and creates a new labial cervical loop stem cell compartment, which produces rapidly growing long tusk-like incisors, and *Lef-1* epithelial overexpression partially rescues the tooth arrest in Sox2 conditional knockout mice. Mechanistically, Pitx2 and Sox2 interact physically and regulate *Lef-1*, *Pitx2* and Sox2 expression during development. Thus, we have uncovered a Pitx2-Sox2-Lef-1 transcriptional mechanism that regulates DESC homeostasis and dental development.

KEY WORDS: Cleft palate, Lef-1, Periderm, Pitx2, Sox2, Stem cells

INTRODUCTION

Regenerative organs, such as peripheral blood, hair follicles, intestine and certain types of teeth, house stem cells that reside in a microenvironment known as the niche. This structure acts as a signaling center to control stem cell fate (Clavel et al., 2012; Lane et al., 2014; Spradling et al., 2001). The precise and timely regulation of stem cell renewal and differentiation is essential for tissue formation, growth and homeostasis over the course of a lifetime (Moore et al., 2006), but the molecular mechanisms

underpinning this regulation are variable and dependent on tissue-specific signaling and transcription factors.

The continuous growth of rodent incisors occurs via the renewal and differentiation of stem cells in both the epithelial and mesenchymal stem cell niches. During mouse incisor development, both dental epithelial and mesenchymal cells are replenished within one month (Smith and Warshasky, 1975). The labial cervical loop (LaCL), which is located at the proximal end of labial side of the incisor, is the stem cell niche for the dental epithelial stem cells (DESCs) (Fig. 1A) (Biehs et al., 2013; Juuri et al., 2012; Thesleff and Tummers, 2009). The neurovascular bundle (NVB) provides a niche in which dental mesenchymal stem cells generate pulp cells and odontoblasts (Kaukua et al., 2014; Zhao et al., 2014). The dental epithelial and mesenchymal components produce signaling factors that promote the differentiation and developmental processes of adjacent tissues.

The transcription factor Sox2 is essential for stem cells and progenitor cells to maintain pluripotency (Boyer et al., 2005; Takahashi and Yamanaka, 2006), and ablation of *Sox2* in mice leads to early mortality after implantation (Avilion et al., 2003). Sox2 has important roles in the development of several endodermal tissues, such as the trachea (Xie et al., 2014) stomach and gut (Que et al., 2007), as well as in ectodermal tissues including the anterior pituitary (Jayakody et al., 2012), lens epithelium (Taranova et al., 2006), tongue epithelium (Arnold et al., 2011) and hair follicles (Clavel et al., 2012). Sox2 was recently identified as a marker for DESCs. Sox2⁺ cells are located in the LaCL and molar cervical loop regions and give rise to the highly proliferative transient-amplifying (TA) cells, which can differentiate into enamel-secreting ameloblasts (Juuri et al., 2012; Li et al., 2015). Conditional inactivation of *Sox2* expression using *Shh^{Cre}* revealed aberrant epithelial morphology in the posterior molars (Juuri et al., 2013). In this study, we identified several molecular mechanisms of *Sox2* in DESC maintenance and proliferation during tooth initiation and growth.

Previous studies have shown the lymphoid enhancer binding factor 1 (Lef-1; also known as Lef1) is regulated by fibroblast growth factor signaling and is required for early tooth development, in which it plays roles in mediating epithelial-mesenchymal interactions (Kratochwil et al., 1996, 2002; Sasaki et al., 2005). *Lef-1* deficiency results in arrested tooth morphogenesis at the late bud stage (van Genderen et al., 1994). Epithelial and mesenchymal tissue recombination assays showed that *Lef-1* is required only transiently in the dental epithelium (Kratochwil et al., 1996). The majority of *Lef-1* expression is shifted to mesenchymal cells/tissues surrounding the epithelium at the bud stage, although *Lef-1* expression persists in the basal cells of the epithelium immediately adjacent to the mesenchyme (Kratochwil et al., 1996;

¹Department of Anatomy and Cell Biology, and the Craniofacial Anomalies Research Center, The University of Iowa, Iowa City, IA 52242, USA. ²Developmental Biology Program, Institute of Biotechnology, University of Helsinki, 00790 Helsinki, Finland. ³State Key Laboratory Breeding Base of Basic Science of Stomatology (Hubei-MOST) and Key Laboratory for Oral Biomedicine of Ministry of Education, School and Hospital of Stomatology, Wuhan University, Wuhan 430079, P.R.China. ⁴Department of Orofacial Sciences and Program in Craniofacial Biology, UCSF, San Francisco, CA 94143-0442, USA. ⁵Iowa Institute for Oral Health Research, College of Dentistry, The University of Iowa, Iowa City, IA 52242, USA. ⁶Department of Obstetrics and Gynecology, The University of Iowa, Iowa City, IA 52242, USA. ⁷Center for Craniofacial Molecular Biology, Ostrow School of Dentistry, University of Southern California, Los Angeles, CA 90033, USA.

*These authors contributed equally to this work

‡Author for correspondence (brad-amendt@uiowa.edu)

© B.A.A., 0000-0001-6524-1006

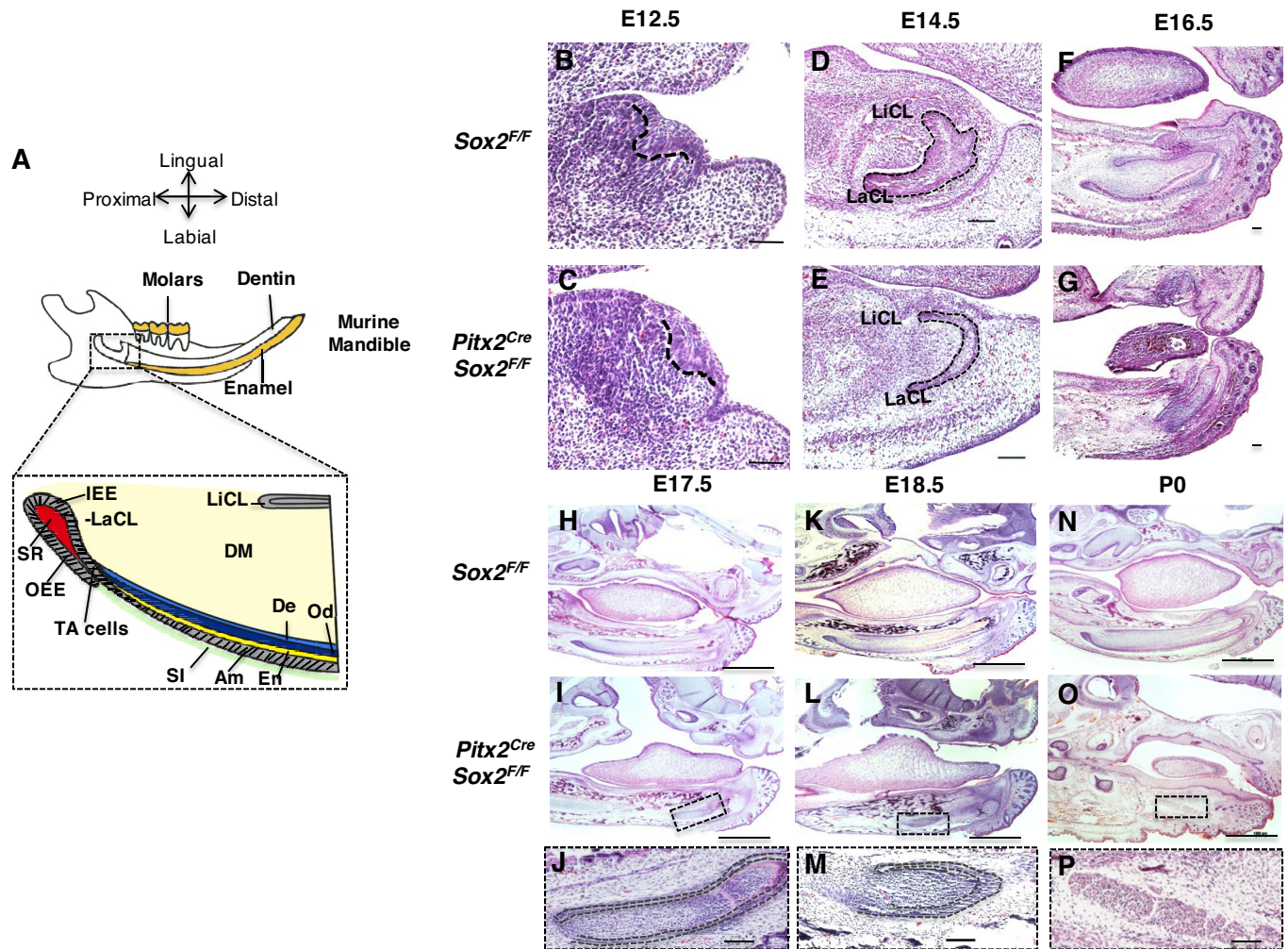


Fig. 1. Loss of *Sox2* in murine embryos causes tooth arrest. (A) Schematic profile of the adult mouse incisor (taken from Biehs et al., 2013 with modifications). The mouse lower incisor comprises a major portion of the mandible. Boxed region depicts the LaCL containing progenitor cells in the stellate reticulum (SR) and the inner (IEE) and outer (OEE) enamel epithelium. Ameloblasts (Am) only appear on the labial side and cause asymmetrical deposition of enamel on labial surface. Dentin (De), produced by odontoblasts (Od), is deposited on both labial and lingual side. DM, dental mesenchyme; En, enamel; SI, stratum intermedium; TA, transient amplifying. (B–G) Hematoxylin and Eosin staining of E12.5, E14.5 and E16.5 embryos (sagittal sections). At E12.5, the tooth bud in *Sox2^{CKO}* embryos (C) is smaller than in control embryos (B). At E14.5 and E16.5, the incisors in *Sox2^{CKO}* embryos (E, G) are smaller in size, have an underdeveloped LaCL and are positioned more towards the anterior region of the mandible, compared with those of control littermates (D, F). Dashed lines delineate dental epithelium. (H–P) Hematoxylin and Eosin staining of E17.5, E18.5 and P0 embryos (sagittal sections). At E17.5 (H), E18.5 (K) and P0 (N) control embryos developed well-formed late bell stage incisors. However, *Sox2^{CKO}* embryos (I, L) only had a remnant of the lower incisor. At P0 the lower incisor was completely absent in *Sox2^{CKO}* mice (O). J, M and P are higher magnifications of boxed regions in I, L and O and show the remnant of incisors (outlined). Scale bars: 100 μ m (B–G, J, M, P); 1 mm (H, I, K, L, N, O).

Sasaki et al., 2005). Both *Sox2* and *Lef-1* are markers of early craniofacial development and are expressed in the oral and dental epithelium (Juuri et al., 2013, 2012; Sasaki et al., 2005; Zhang et al., 2012), but potential *Sox2-Lef-1* genetic interactions remain unexplored.

A role for *Sox2* in DESC maintenance and proliferation during tooth formation has been proposed by conditionally ablating *Sox2* in the oral and dental epithelium using the *Pitx2^{Cre}* system. Conditional inactivation of *Sox2* expression in craniofacial tissues leads to severe craniofacial defects, including cleft palate, and arrested incisor development. We report that the *Pitx2^{Cre}/Sox2^{F/F}* (*Sox2^{CKO}*) dental defects are due to impaired stem cell proliferation and defective dental epithelial cell differentiation. Because *Lef-1* is also required for tooth development and potentially stem cell proliferation, we generated a *Lef-1* conditional overexpression mouse and used *Pitx2^{Cre}* to overexpress *Lef-1* in the oral and dental

epithelium. We hypothesized that *Lef-1* could act as a stem cell factor to induce progenitor cell proliferation and incisor self-renewal. In fact, *Lef-1* overexpression formed a new DESC compartment. Furthermore, *Lef-1* overexpression partially rescued the incisor phenotype in *Sox2^{CKO}* mice. Based on our previous reports and new *in vitro* data, the interaction of *Pitx2* and *Sox2* regulates *Lef-1*, *Pitx2* and *Sox2* expression. In this article, we will provide evidence suggesting a *Pitx2-Sox2-Lef-1* regulatory mechanism for DESC maintenance and proliferation.

RESULTS

Specific ablation of *Sox2* in the oral and dental epithelium

Consistent with previous reports (Avilion et al., 2003; Ellis et al., 2004), we found that *Sox2* is expressed in the lateral ventricle and epithelial tissues in craniofacial regions of embryonic day (E)18.5 wild-type embryos, including the nasal epithelium, oral epithelium,

tongue epithelium and dental epithelium (Fig. S1A,B). As it was previously shown (Juuri et al., 2012), we also detected specific expression of Sox2 in the labial cervical loop (LaCL), where the DESCs reside (Fig. S1C).

To investigate the function of *Sox2* in the oral and dental epithelium, we generated *Pitx2^{Cre}-Sox2^{F/F}* mice, hereafter referred to as *Sox2^{cKO}* mice. We have previously shown that *Pitx2* is expressed in the oral ectoderm at E10.5 and later stages and that *Pitx2^{Cre}* mice have normal craniofacial and early tooth development (Cao et al., 2010; Li et al., 2013). *Pitx2^{Cre}* has robust and specific expression in the dental, oral and tongue epithelium at E11.5 and E14.5 (Fig. S1D,E). Immunofluorescence staining demonstrates that Sox2 was efficiently ablated in the lower incisor LaCL and oral epithelium but not in the lateral ventricle of *Sox2^{cKO}* mice (Fig. S1F–M). These data demonstrate the specificity of the *Pitx2^{Cre}*, which is not expressed in the lateral ventricle.

Inactivation of Sox2 leads to lower incisor arrest at E16.5 and abnormalities in upper incisor and molar development

The first step of mouse tooth development is a thickening of ectoderm-derived oral epithelium at E11.5, after which the thickened epithelium invaginates into the underlying cranial neural crest-derived mesenchyme to form a tooth bud at E12.5. At the bud stage, *Sox2^{cKO}* tooth germs were detectable but displayed a slightly delayed invagination compared with those of littermate control embryos (Fig. 1B,C). At E14.5, the tooth epithelium further invaginates to envelop the mesenchymal dental papilla to form a cap stage incisor. The cap stage incisors are longitudinally oriented in the mandible with a cervical loop in the labial (LaCL) and lingual (LiCL) epithelium (Fig. 1A). The LaCL was smaller in *Sox2^{cKO}* embryos at this stage and the lower incisor was positioned more anteriorly and associated with the oral epithelium compared with control incisors (Fig. 1D,E). At E16.5, the *Sox2^{cKO}* incisors were smaller, invagination was hindered and the LaCL was severely underdeveloped and lacking structure, compared with *Sox^{F/F}* littermates (Fig. 1F,G). At E17.5 and E18.5, lower incisor development regressed in *Sox2^{cKO}* embryos (Fig. 1H–M), until it was no longer detectable at postnatal day (P)0 (Fig. 1N–P).

Sox2 is also expressed in upper incisors and molars and *Shh^{Cre}-Sox^{F/F}* mice exhibit molar defects (Juuri et al., 2013). We found that the upper incisors and molars in *Sox2^{cKO}* embryos were smaller and associated with delayed invagination at E14.5 (Fig. S2A,B). At E16.5, *Sox2^{cKO}* molars also exhibited an abnormal shape and upper incisors showed a delay in rotation (Fig. S2C). At P0, *Sox2^{cKO}* molars lacked cusps (Fig. S2D). These data indicate a role for *Sox2* in dental epithelial cell proliferation and tooth growth.

Sox2 was conditionally deleted using the *Krt14^{Cre}* but we found no obvious incisor defects, although *Krt14^{Cre}-Sox2^{F/F}* mice exhibited a mild molar defect (Fig. S3). This defect included an expanded dental lamina starting at E13.5 (Fig. S3B,E,H,K,N,Q) and absence of the third molar (data not shown). Interestingly, the pattern of *Shh* and *Fgf4* expression was slightly expanded in E14.5 *Krt14^{Cre}-Sox2^{F/F}* molars (Fig. S3T,V), suggesting that *Sox2* might repress *Shh* and *Fgf4* expression.

Sox2 regulates incisor growth in adult mice

Sox2^{cKO} mice die at birth, similar to other *Sox2* conditional knockout mice (Juuri et al., 2013; Zhang et al., 2012). To determine whether *Sox2* plays a role in adult incisor growth, *Sox2^{F/F}* mice were crossed with *Rosa26^{CreERT}* mice in which *Cre* expression can be induced by tamoxifen. After treatment with tamoxifen, we cut the left lower incisors of control and *Rosa26^{CreERT}-Sox2^{F/F}* mice

(Fig. 2A,B). Five days after injury, incisors of tamoxifen-treated control mice grew to a length comparable to the uninjured right lower incisor. By contrast, incisors of tamoxifen-treated *Rosa26^{CreERT}-Sox2^{F/F}* mice exhibited severely reduced growth, an approximate 50% decrease compared with control mice (Fig. 2B,C). We confirmed that Sox2 expression was ablated in tamoxifen-treated mice by immunofluorescence staining (Fig. 2B).

Sox2 ablation leads to reduced stem cell proliferation

Because the loss of *Sox2* expression caused embryonic incisor developmental arrest and reduced growth of the adult lower incisor, we next examined proliferation of cells in the LaCL. Immunofluorescence staining of Ki67 (also known as Mki67) in E16.5 *Sox2^{cKO}* embryonic incisors showed a smaller LaCL and decreased stem cell proliferation in the LaCL compared with control embryos (*Sox2^{F/F}*) (Fig. 3A–B'). Quantitative analysis indicated that the percentage of Ki67-positive cells was decreased by 40% in *Sox2^{cKO}* LaCLs (Fig. 3C), suggesting that progenitor cell proliferation was inhibited by loss of *Sox2*. However, no change in proliferation was detected in the LiCL of the *Sox2^{cKO}* embryos compared with controls (Fig. 3A'',B'',C). As a comparison, we detected no change in cell proliferation in *Pitx2^{Cre}/Sox2^{F/+}* mice (Fig. S4A–C), indicating that the defect is not due to the *Pitx2^{Cre}* allele.

To determine whether altered progenitor cell proliferation could contribute to reduced incisor growth in *Sox2^{cKO}* embryos, we performed thymidine analog double labeling in control and *Sox2^{cKO}* mouse mandibles. In this experiment, highly proliferative cells sequentially incorporate two different thymidine analogues, 5-chloro-2'-deoxyuridine (CldU) and 5-iodo-2'-deoxyuridine (IdU), which allow us to observe and quantify two successive rounds of cell division and potential migration. There were relatively fewer IdU⁺ cells observed in *Sox2^{cKO}* LaCL compared with control embryos 1 hour after IdU injection (Fig. 3D,E, green), indicating decreased cell proliferation in *Sox2^{cKO}* LaCL. There were no IdU-labeled cells in the distal tip of the incisors (Fig. 3D,D'',E,E''). At 24 h after injection of CldU, the dental epithelial cells in both the proximal region and distal region of control embryos (*Sox^{F/F}*) are labeled with CldU (Fig. 3D,D', red), but there were fewer CldU⁺ cells in the distal tip of *Sox2^{cKO}* incisor, suggesting that DESC/progenitor cell migration was affected by loss of *Sox2* (Fig. 3E,E',F).

It is possible that reduced growth in the *Sox2^{cKO}* lower incisor was caused by increased cell death. However, TUNEL staining and immunohistochemistry staining of an early cell death marker, cleaved caspase-3, revealed no obvious cell apoptosis in either *Sox2^{F/F}* or *Sox2^{cKO}* incisors (Fig. S4D–K). Therefore, these data suggest that *Sox2* primarily regulates progenitor cell proliferation in the LaCL, but the loss of *Sox2* in DESCs does not affect the rate of cell death.

Sox2 and Lef-1 epithelial expression domains are juxtaposed in the mouse oral epithelium and dental placode

In the *Sox2^{cKO}* embryos, tooth development is halted at the late bud-bell stage and, interestingly, in *Lef-1* null mice dental development is arrested at the late bud stage. To determine whether *Sox2* and *Lef-1* interact, we analyzed *Sox2* and *Lef-1* protein expression in E11.5 wild-type (WT), *Sox2^{F/F}* and *Sox2^{cKO}* incisors at the dental placode stage (Fig. 4A). *Sox2* and *Lef-1* were both expressed in the oral epithelium and dental placode of both lower and upper incisors of E11.5 WT embryos (Fig. 4B,C). However, *Lef-1* expression was detectable in the anterior regions of the upper and lower incisors,

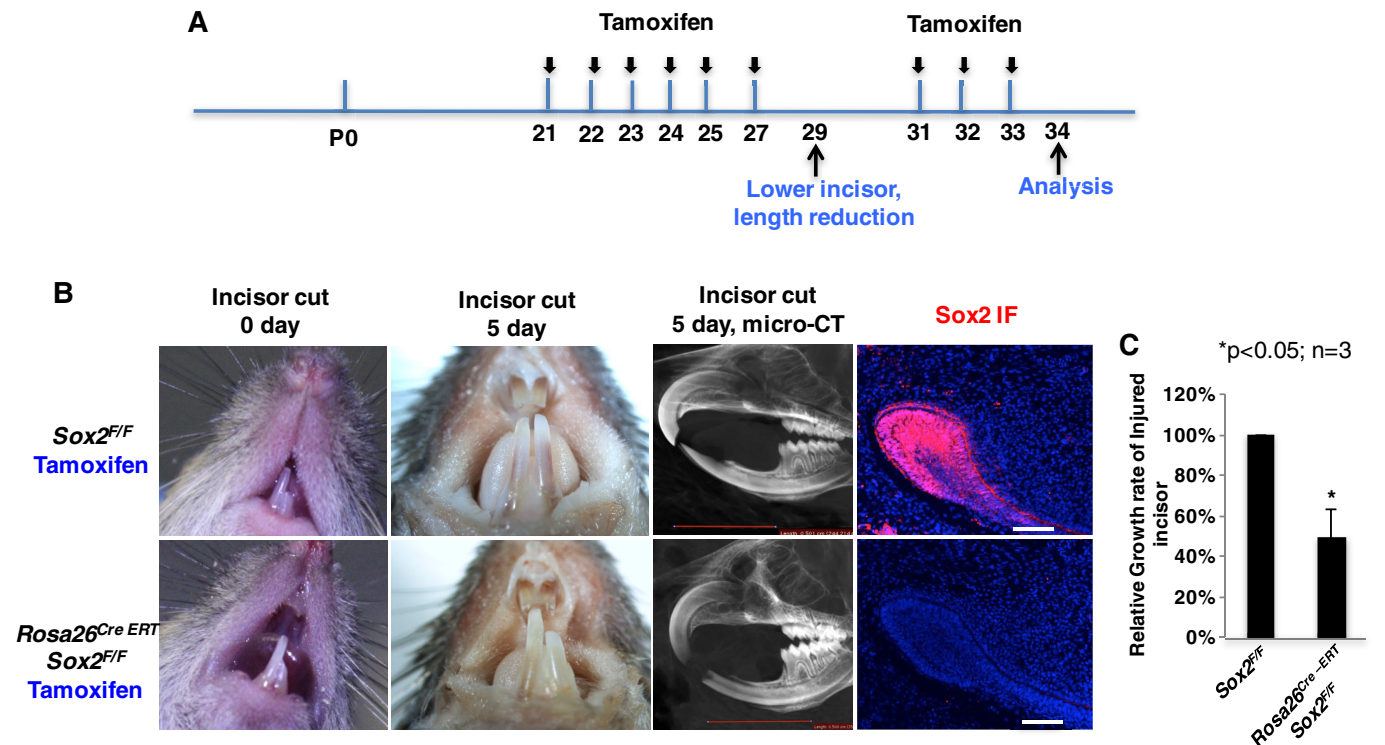


Fig. 2. Deletion of Sox2 in adult mice inhibits incisor regeneration. (A) Tamoxifen treatment, tooth length reduction and histological analysis time line in *Sox2^{F/F}* control and *Rosa26^{Cre-ERT}/Sox2^{F/F}* mice. (B) Images of P29 and P34 mouse incisors after tamoxifen treatment and cutting of the left lower incisor. First column: mouse incisors after cutting half of the left lower incisor. Second column: mouse incisors 5 days after shortening. Third column: microcomputed tomography (μ CT) analysis of shortened incisors after 5 days of recovery. Fourth column: Sox2 expression visualized by immunofluorescence (IF) in tamoxifen-treated *Rosa26^{CreERT}/Sox2^{F/F}* and control mice. (C) Quantification data (mean \pm s.e.m.) of the relative growth rate of the shortened incisor in *Sox2^{F/F}* and *Rosa26^{CreERT}/Sox2^{F/F}* mice after treatment with tamoxifen. Scale bars: 5 mm (μ CT images); 100 μ m (IF images).

whereas Sox2 expression was detectable in the posterior region of the incisors (Fig. 4D,E). At E12.5, the pattern of Sox2 and Lef-1 expression were similar to E11.5 as the dental epithelium invaginates into the surrounding mesenchyme (Fig. 4F). As expected, E11.5 *Sox2^{F/F}* embryos were indistinguishable from WT (Fig. 4E,H–J). Although Sox2 expression was undetectable in *Sox2^{ckO}* embryos at E11.5, Lef-1 expression was not affected (Fig. 4L–N). Notably, the incisor placodes in *Sox2^{ckO}* E11.5 embryos also showed delayed epithelial thickening at this stage (Fig. 4K).

To understand further the anterior/posterior expression patterns, coronal sections of E11.5 WT embryos were analyzed for Lef-1 and Sox2 protein expression (Fig. S5A, schematic). Sox2 was expressed in the posterior domain of the lower incisor and Lef-1 was expressed in the anterior region (Fig. S5B, arrowheads showing incisor placodes). Sox2 expression in the molar was localized to the posterior regions and Lef-1 expression was observed in the anterior region on the mandible (Fig. S5B). These results suggest that Sox2 and Lef-1 may act independently of each other to regulate incisor development.

Conditional overexpression of Lef-1 creates a new LaCL stem cell niche and abnormal ‘tusk-like’ incisors

To determine the effect of continuous *Lef-1* expression during incisor development, we generated a *Lef-1* conditional overexpression mouse. A *Lef-1* full-length isoform construct was preceded by a *loxP*-flanked ‘STOP’ and inserted into the *Rosa26* locus, to make a *Cre*-responsive *Lef-1* conditional knock-in mouse (*Lef-1^{ckI}*) (Fig. 5A). *Lef-1^{ckI}* mice were crossed with *Pitx2^{Cre}* mice to drive

the overexpression of *Lef-1* in the dental and oral epithelium (Fig. 5A). *Lef-1* immunostaining confirmed the overexpression of *Lef-1* in the dental epithelium of the conditional overexpression *Pitx2^{Cre}-Lef-1^{ckI}* embryos (hereafter termed *COEL*) (Fig. S6C). The *COEL* mice developed long, thick tusk-like incisors compared with *Lef-1^{ckI}* mice (control) (Fig. 5B,C). Microcomputed tomography (μ CT) analysis of 3-month-old mice revealed that both upper and lower incisors in *COEL* mice underwent rapid growth compared with *Lef-1^{ckI}* mice (Fig. 5D,E). The LaCL in the lower incisors of E16.5 *COEL* embryos were larger than those of control embryos and included a new cell compartment forming on the labial side (Fig. S6A). At P0, the sizes of control and *COEL* lower incisors were comparable, but an extra branch of the LaCL was detectable in *COEL* embryos (Fig. S6B).

To determine whether the cells in the branched LaCL of *COEL* mice are dental epithelial stem cells, we analyzed Sox2 expression in P1 control and *COEL* LaCL regions. The LaCL and the branched region both contained Sox2-positive stem cells (Fig. 5F,G), suggesting that overexpression of Lef-1 resulted in a new cluster of stem cells. Three-dimensional reconstruction shows the structure of the expanded LaCL with multiple layers and a branching stem cell niche (Fig. 5H–K). Previous studies on tusk-like incisors in *Spry4^{-/-}*; *Spry2^{+/-}* mice (Klein et al., 2008) revealed that overgrowth of the lower incisor could be due to ectopic deposition of lingual enamel. To test whether *Lef-1* overexpression produced ectopic enamel formation, we performed amelogenin immunostaining in E18.5 embryos and found elevated amelogenin expression in the labial side of *COEL* LIs, but no ectopic amelogenin expression was detected in the lingual side of *COEL* incisors (Fig. S6D).

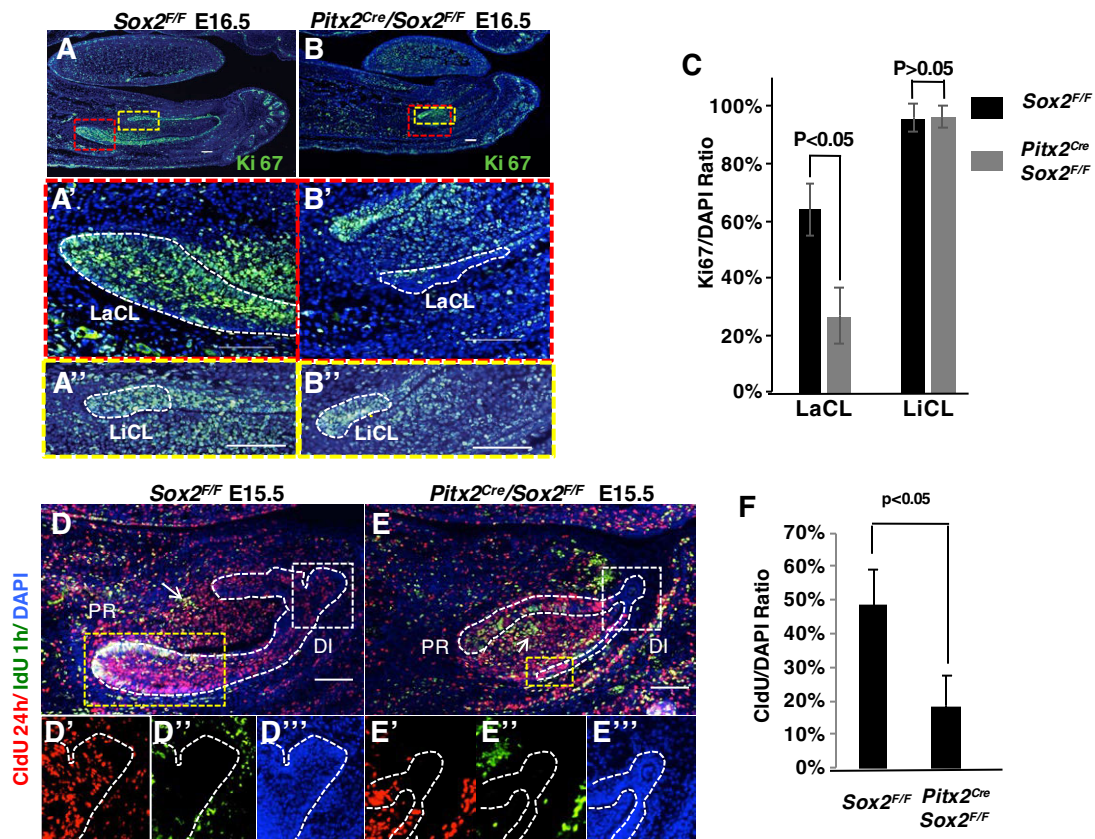


Fig. 3. Sox2 regulates dental epithelial stem cell proliferation and differentiation. (A–B^{''}) Immunofluorescence staining of the proliferation marker Ki67 in sagittal sections of E16.5 *Sox2^{F/F}* and *Sox2^{CKO}* mouse incisors. (A', B') High magnification view of red boxed regions in A and B to show the proliferation in the LaCL (outlined). (A'', B'') High magnification view of white boxed regions in A and B to show the proliferation in the LiCL (outlined). (C) Quantification of the ratio of Ki67-positive cells to total cells in the cervical loops. Mean \pm s.e.m., $n=3$. (D–F) Progenitor cell differentiation measured using two different labels (CldU and IdU), which were injected and measured after 24 h and 1 h, respectively. The red label-retaining cells (CldU) mark differentiated cells and the green label-retaining cells (IdU) mark recently mitotic cells. The arrows indicate the region of neural vascular bundles. The LaCLs are highlighted by yellow dashed boxes. (D'–D''', E'–E''') Higher magnifications of the white boxed areas in D and E, respectively, highlight the progenitor cells at the distal tip of the incisors. DI, distal; PR, proximal. (F) Quantification of CldU⁺ cells in the epithelial tissue of the white boxed region shown in D' and E'. Mean \pm s.e.m., $n=3$. Scale bars: 100 μ m.

We next investigated whether increased stem cell proliferation in the LaCL could contribute to the increased growth of incisors in *COEL* mice. BrdU (5-bromo-2'-deoxyuridine) labeling of cells in the E18.5 *COEL* LaCL showed a 15% increase in progenitor cell proliferation compared with the control LaCL (Fig. 5L,M). However, at P1, proliferation in the LaCL regions was similar between control and *COEL* neonates (Fig. 5N), but the total number of stem cells was increased by 20% in the *COEL* LaCL (Fig. 5O). Most of the cells in the *COEL* branched LaCL region were not labeled with BrdU, suggesting that these cells were quiescent, i.e. not undergoing proliferation (Fig. 5N). These data point to a model in which overexpression of *Lef-1* in the incisor results in increased cell proliferation at embryonic stages and formation of a new compartment of stem cells in the LaCL, which facilitates incisor growth and the formation of tusk-like incisors.

Lef-1 overexpression rescues tooth arrest in *Sox2^{CKO}* embryos

Because both *Sox2* and *Lef-1* appear to control dental epithelial stem cell renewal and maintenance, we next investigated whether *Lef-1* overexpression could rescue the tooth arrest in *Sox2^{CKO}* embryos. To test our hypothesis, we crossed *Sox2^{CKO}* mice with *COEL* mice to produce *Pitx2^{Cre}/Sox2^{F/F}/Lef-1^{CKI}* (rescue) mice. At E18.5, the *Sox2^{F/F}/Lef-1^{CKI}* (control) embryos developed well-formed late bell

stage incisors (Fig. 6A). The E18.5 *Sox2^{CKO}* embryos had a remnant of the LI at this stage (Fig. 1K,L). In rescue mice, the LIs are detectable, but the LI was positioned at the anterior region of the mandible and was smaller in size (Fig. 6B). The forward positioning of the LI might be due to oral adhesions that remain. The LaCL in rescue mice was smaller than in control embryos (Fig. 6B). In the labial side of control embryos, the lower incisors develop three layers: odontoblasts, ameloblasts and the stratum intermedium. However, there was only one layer of cells in rescue embryos, suggesting that differentiation was blocked (Fig. 6A,B, blue boxes). Interestingly, the LaCL was partially restored in the rescue embryos (Fig. 6A,B, black boxes). We also examined P0 rescue incisors and found similar phenotypes (Fig. S7).

To confirm the effect on differentiation in rescue embryos, we analyzed ameloblast differentiation by immunofluorescence using an antibody against amelogenin, a marker for differentiated dental epithelial cells, in E18.5 lower incisors. In control mice, amelogenin was expressed in the labial side (Fig. 6C,C'). However, amelogenin was ectopically expressed on the lingual side of the lower incisor in rescue embryos (Fig. 6D,D'). *Lef-1* is highly expressed in the lingual cervical loop at E18.5 due to *Pitx2^{Cre}* activity in these mice (Fig. 6E,F). Thus, we speculate that the interplay between *Sox2* and *Lef-1* with other factors specifies asymmetric amelogenin expression.

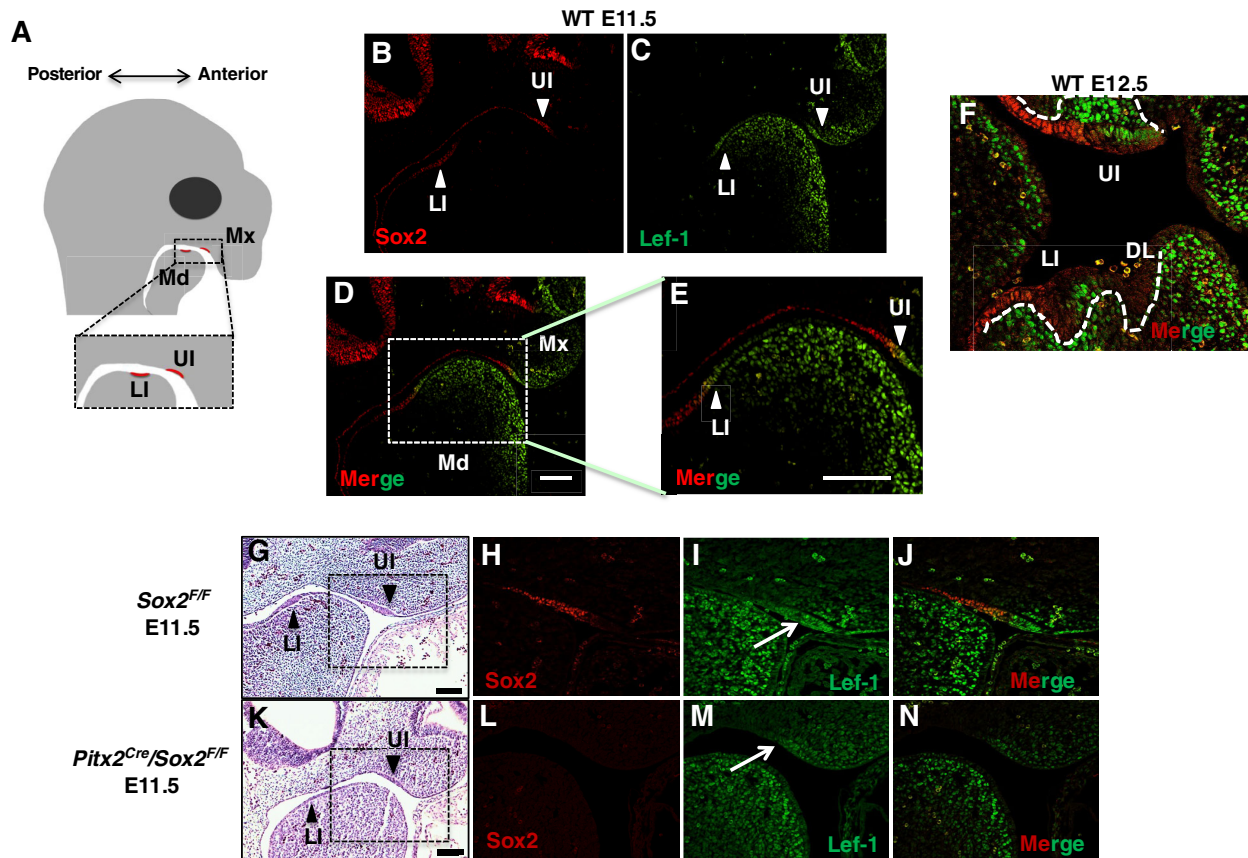


Fig. 4. Sox2 and Lef-1 expression domains are juxtaposed in the dental placode and oral epithelium. (A) Schematic of an E11.5 mouse head shows upper and lower dental placodes. (B,C) Sox2 and Lef-1 immunofluorescence staining in E11.5 wild-type (WT) embryos. (D) Merged image of Sox2 and Lef-1 staining in E11.5 WT showing the juxtaposed expression domains of these two factors. (E) Higher magnification of the boxed region in D. Arrows indicate position of the lower and upper incisor dental placodes. (F) Double immunofluorescence staining of Sox2 (red) and Lef-1 (green) in E12.5 WT embryos, showing specific expression domains of each factor in the developing incisor tooth buds. Dashed lines mark boundary between dental epithelium and mesenchyme. (G,K) Hematoxylin and Eosin staining of E11.5 *Sox2^{F/F}* and *Sox2^{ckO}* embryos; arrows point to the LI and UI dental placodes. (H–J,L–N) Sox2 expression is absent in the *Sox2^{ckO}* embryos; however, Lef-1 expression is not affected compared with controls (higher magnification of boxed regions in G and K). Arrows in I and M highlight the Lef-1 expression. DL, dental lamina; LI, lower incisor; Md, mandible; Mx, Maxilla; UI, upper incisor. Scale bars: 100 μ m.

To determine whether progenitor cell proliferation was rescued and contributes to the development of the LI in rescue mice, we analyzed proliferation at E16.5. Proliferation was dramatically reduced in the LI LaCL region in *Sox2^{ckO}* mice, but it was restored in rescue embryos (Fig. 6G,H). Thus, overexpression *Lef-1* in *Sox2*-ablated incisors partially rescued the tooth arrest by promoting stem cell maintenance and cell proliferation.

We next investigated whether *Lef-1* overexpression affected Sox2 expression in the *COEL* and rescue E11.5 embryos. Lef-1 expression was not changed in the *Pitx2^{Cre}/Sox2^{F/F}* embryos and Sox2 expression was unchanged in the *COEL* embryos; however, Lef-1 expression was expanded posteriorly in the rescue embryos (Fig. S8A). We also asked whether *Pitx2* expression was affected in the *Pitx2^{Cre}/Sox2^{F/+}* embryos. *Pitx2* expression was detected by *in situ* hybridization and in the *Pitx2^{Cre}/Sox^{F/+}* E11.5 embryos *Pitx2* expression was slightly increased compared with *Sox2^{F/F}* embryos owing to the reduced expression of Sox2 (Fig. S8B); we show in later experiments that Sox2 interacts with Pitx2 to inhibit transcriptional activation of *Pitx2* expression, thus decreased Sox2 expression would increase *Pitx2* expression. Interestingly, because *Pitx2^{Cre}* embryos have only one functional allele of *Pitx2*, the lack of a decrease in *Pitx2* expression indicates that the loss of a *Pitx2* allele in the *Pitx2^{Cre}* mouse does not contribute to the defects in the *Sox2^{ckO}* embryos.

Additionally, Sox2 expression was expanded in the LaCL of *COEL* E18.5 embryos and specifically in the new stem cell compartment (Fig. S8D, arrowhead). The new stem cell compartment showed less Lef-1 expression compared with the complete LaCL (Fig. S8D, merge). Thus, Lef-1 overexpression created a new stem cell compartment but the compartment contained Sox2-positive cells that were not proliferating (Fig. 5N).

Sox2 attenuates Pitx2 transcriptional activation of Lef-1, Sox2 and Pitx2 through direct protein interactions

To determine a molecular mechanism for the Sox2-Lef-1 effects on incisor development, we focused on the transcriptional activities of these factors in concert with Pitx2. Pitx2 is the first transcriptional marker of tooth development and *Pitx2* null mice have tooth development arrest at E12.5 (Liu et al., 2003; Lu et al., 1999). We have previously shown that Pitx2 regulates *Lef-1* expression during odontogenesis (Amen et al., 2007; Vadlamudi et al., 2005). RNA-sequencing data showed that Sox2 expression was upregulated in the mandibles of *Pitx2* overexpression mice and downregulated in the mandibles of *Pitx2* null mice (B.A. and H. Cao, unpublished data), indicating that Pitx2 regulates Sox2. Sequence analyses of the *Sox2* promoter identified one Pitx2-binding element located in the 5'UTR and another in a distal element 845 bp upstream of the transcription start site (TSS) (Fig. S9A). Chromatin-immunoprecipitation (ChIP)

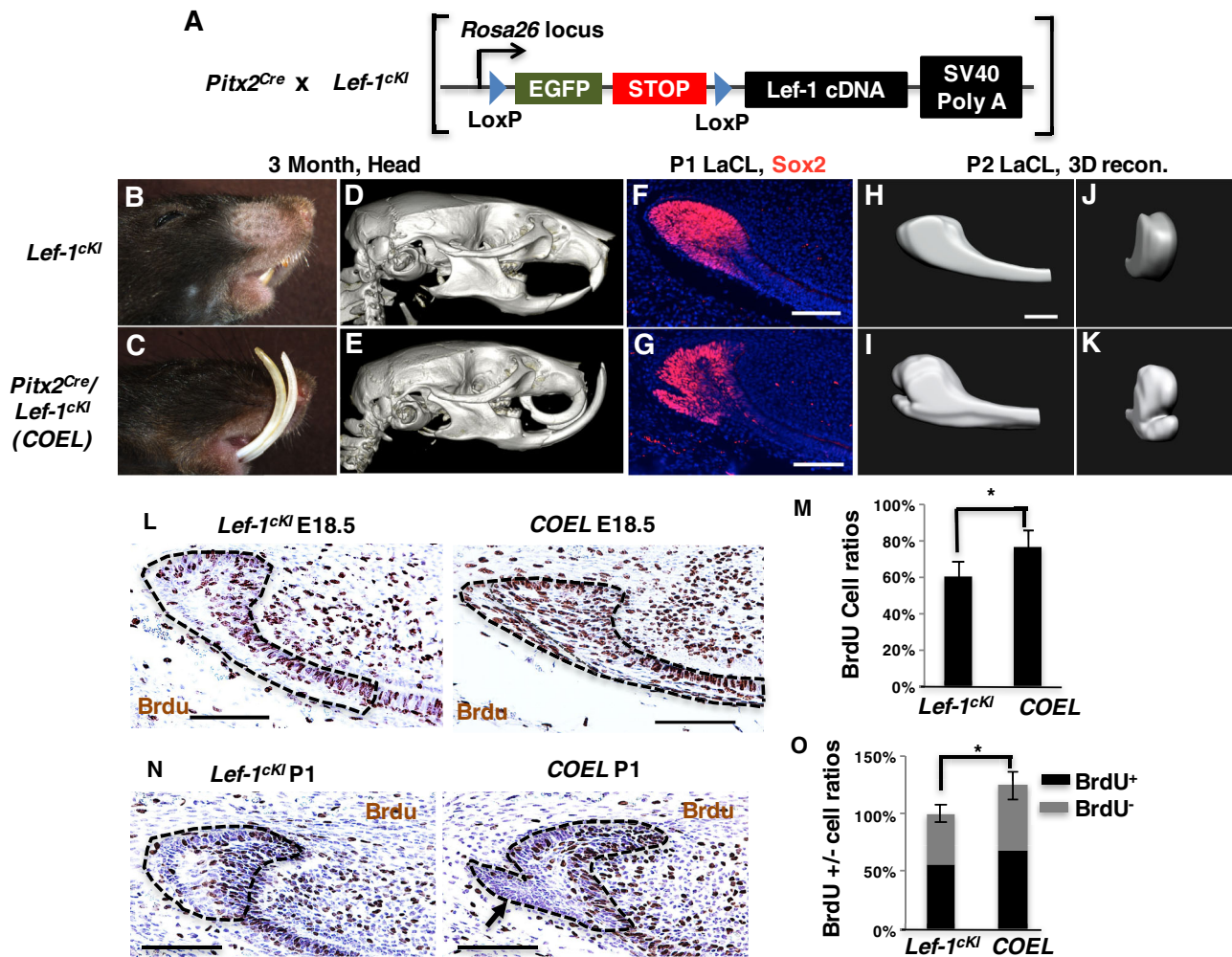


Fig. 5. Conditional overexpression of *Lef-1* (COEL) results in tusk-like incisors, creation of a new stem cell compartment in the LaCL and increased dental epithelial stem cell proliferation. (A) Schematic of the *Lef-1* conditional overexpression cassette used to generate the COEL mouse. (B, C) Heads showing overgrown incisors from 3-month-old *Lef-1^{cKI}* (*Lef-1* conditional knock-in, control) and *Pitx2^{Cre}/Lef-1^{cKI/cKI}* (*Lef-1* overexpression, COEL) mice. (D, E) µCT analysis of the mouse heads shown in B and C. Both the upper and lower incisors are overgrown in COEL mice. (F, G) Immunofluorescence staining of *Sox2* in the LaCL of P1 control and COEL incisors. Note the extra stem cell compartment in the LaCL of COEL mice. (H–K) 3D composites of the LI LaCL comparing WT (*Lef-1^{cKI}*) with the COEL LI at P2. (L) BrdU labeling of the E18.5 control and COEL incisors. (M) Quantification of the percentage of BrdU⁺ cells in the E18.5 LaCL of control and COEL incisors. Mean ± s.e.m., *n*=3. (N) BrdU labeling of P1 control and COEL lower incisors. Note the lack of proliferative cells in the extra stem cell compartment (arrow). (O) Quantification of BrdU-positive compared with BrdU-negative cells as a ratio of all cells in the LaCL. Mean ± s.e.m., *n*=3. **P*<0.05. Scale bars: 100 µm.

showed *Pitx2* binding to both elements (Fig. S9B,C). We also identified a putative *Sox2*-binding element 1972 bp upstream of the *Sox2* TSS and ChIP assay showed that *Sox2* binds to this element (Fig. S9D–F).

The *Sox2* promoter (4.0 kb) was cloned into a luciferase vector and transfected into LS-8 oral epithelial cells to test for regulation by *Pitx2* and *Sox2*. *Pitx2* activated the *Sox2* promoter 15-fold compared with empty vector and *Sox2* activated its own promoter threefold (Fig. S9G). However, *Sox2* repressed *Pitx2* activation of the *Sox2* promoter from 15-fold activation to fivefold (Fig. S9G). This repression of *Pitx2* transcriptional activity was not promoter specific as *Sox2* repressed *Pitx2* activation of the *Lef-1* and *Pitx2* promoters (Fig. S9G). To confirm this regulation, we measured endogenous levels of *Sox2*, *Lef-1* and *Pitx2* in LS-8 cells transfected with empty vector (pcDNA3.1), *Pitx2* or *Sox2*. Cells transfected with *Pitx2* show significantly increased levels of *Sox2* and *Lef-1* transcripts (Fig. S9H), whereas the cells transfected with *Sox2* showed no significant difference in the levels of *Lef-1* or *Pitx2* (Fig. S9H).

Finally, we show, using immunoprecipitation (IP) assays, that *Pitx2* and *Sox2* interact endogenously (Fig. S10A). We further conclude that the HMG domain and the C terminus in *Sox2* protein mediate the *Pitx2* binding to *Sox2* based on results from a glutathione S-transferase (GST) pull-down assay (Fig. S10B–D).

Taken together, our results show that *Sox2* protein and *Pitx2* protein interact to repress *Pitx2* transcriptional activity. These findings provide a new mechanism to establish the juxtaposed expression domains of *Sox2* and *Lef-1* during tooth development. *Pitx2* is expressed throughout the oral epithelium and dental placode. In the posterior region of the dental placode, *Pitx2* activates *Sox2* and the *Pitx2*-*Sox2* complex inhibits *Lef-1* expression. In the anterior region of the dental placode, the absence of *Sox2* is in this region allows *Pitx2* activation of *Lef-1*. A working model of this new transcriptional regulation and expression of *Sox2* and *Lef-1* is presented in Fig. 7. At later stages of incisor development in the LaCL, *Lef-1* is not expressed in the dental epithelium but shifts to the adjacent mesenchyme. We demonstrate that a *Pitx2*-*Sox2*-*Lef-1*

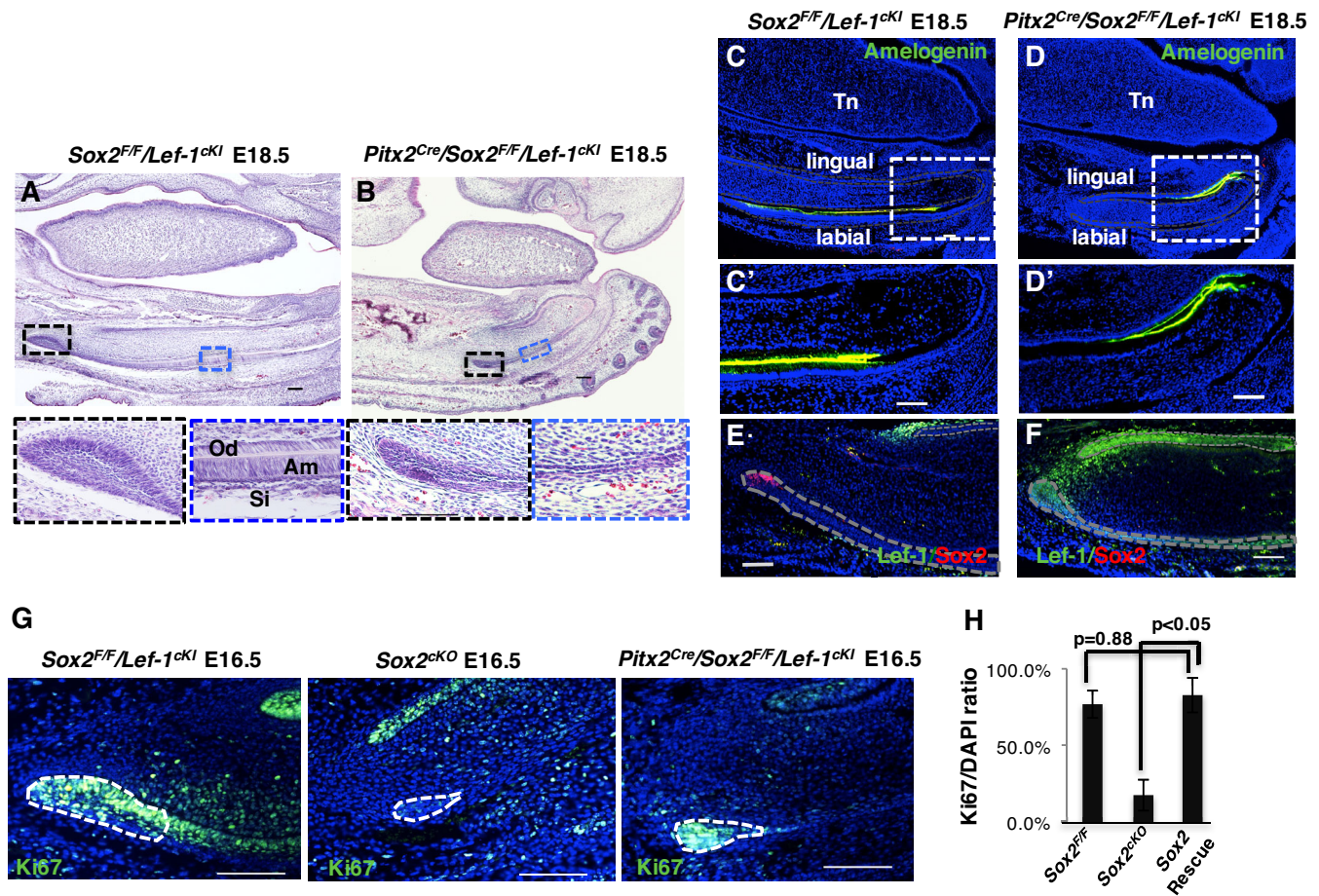


Fig. 6. Overexpression of *Lef-1* partially rescues tooth arrest in *Sox2^{cKO}* embryos. (A,B) Hematoxylin and Eosin staining of sagittal sections of E18.5 *Sox2^{F/F}Lef-1^{ckI}* (control) and *Pitx2^{Cre}Sox2^{F/F}Lef-1^{ckI}* (rescue) mandibles and maxilla. Differentiation of the labial dental epithelial cells (Am and Si) and adjacent odontoblast (Od) cells in the rescue incisors is highlighted in the blue boxes (higher magnification shown below). Black boxes show the LaCL is present in rescue embryos but much smaller than in control incisors (higher magnification shown below). Am, ameloblast; Od, odontoblast; Si, stratum intermedium. (C–D') Amelogenin immunofluorescence staining in E18.5 control and rescue incisors revealed that amelogenin expression was switched to the lingual side in the rescue incisor compared with the labial expression in the control. Boxed regions in C and D are shown at higher magnification in C' and D', respectively. (E,F) Sox2 and Lef-1 double immunostaining in E18.5 control and rescue incisors. Dental epithelial cells are outlined. (G) Proliferation as determined by the marker Ki67 was reduced in the *Sox2^{cKO}* E16.5 LaCL (outlined) but was restored in the rescue embryos compared with controls. (H) Proliferation of the cells in the LaCL was quantified by comparison of Ki67-stained (proliferating) cells versus DAPI-stained (total) cells. Mean±s.e.m., $n=3$. Scale bars: 100 μ m.

regulatory mechanism plays a major role in maintaining the stem cell niche and promoting stem cell proliferation (Fig. 7).

DISCUSSION

Previous studies have shown an early role for *Sox2* in the specification of DESCs, and *Sox2⁺* cells mark DESCs (Juuri et al., 2012; Li et al., 2015). Furthermore, conditional deletion of *Sox2* using *Shh^{Cre}* results in abnormal epithelial growth in mouse molars (Juuri et al., 2013), consistent with what we observed in *K14^{Cre}-Sox2^{F/F}* embryos. However, by using the earliest dental epithelium marker, *Pitx2^{Cre}*, to ablate *Sox2* in the dental and oral epithelium, we found that the loss of *Sox2* leads to incisor developmental arrest at E16.5 with a complete disintegration at P0 and abnormal molar growth. We propose that this is mainly due to the failure to maintain the DESC niche at an early stage resulting in a lack of proliferative cells and gradual loss of the incisor tooth germ. These data correlate well with the role of *Sox2* in the specification of the stem cell niche (Juuri et al., 2012). Furthermore, loss of *Sox2* during adult lower incisor growth resulted in a reduction of incisor regeneration, demonstrating an essential role for *Sox2* in maintaining the adult DESC niche. Therefore, these studies show

that incisor arrest at E16.5 and abnormal molar formation is due to depletion of the epithelial stem cells in the LaCL, which is regulated by *Sox2*.

Lef-1 controls stem cell self-renewal and establishes stem and progenitor cell compartments in mouse epidermis and hair follicles (Huang and Qin, 2010; Lowry et al., 2005; Petersson et al., 2011). In our study, *Lef-1* overexpression enhanced DESC production and promoted stem cell proliferation but also produced a new compartment of mitotically inactive stem cells in the LaCL leading to dramatically increased growth of the incisor. Thus, *Lef-1* activity contributes to the establishment of stem and progenitor cell compartments in the mouse incisor. *Sox2* and *Lef-1* expression domains define the epithelial component of the initial dental placode, demonstrating distinct roles for these two factors. It appears that *Sox2* and *Lef-1* control different cell subpopulations in the developing tooth germ. In support of this, *Lef-1* overexpression increased the number of cells in the LaCL, but, interestingly, the branched 'new' stem cell compartment contained predominantly *Sox2⁺* cells that were not BrdU labeled, suggesting that these cells were quiescent cells. A possible explanation is that the proliferating cells expressing *Lef-1* in the lower incisor LaCL are an expanded

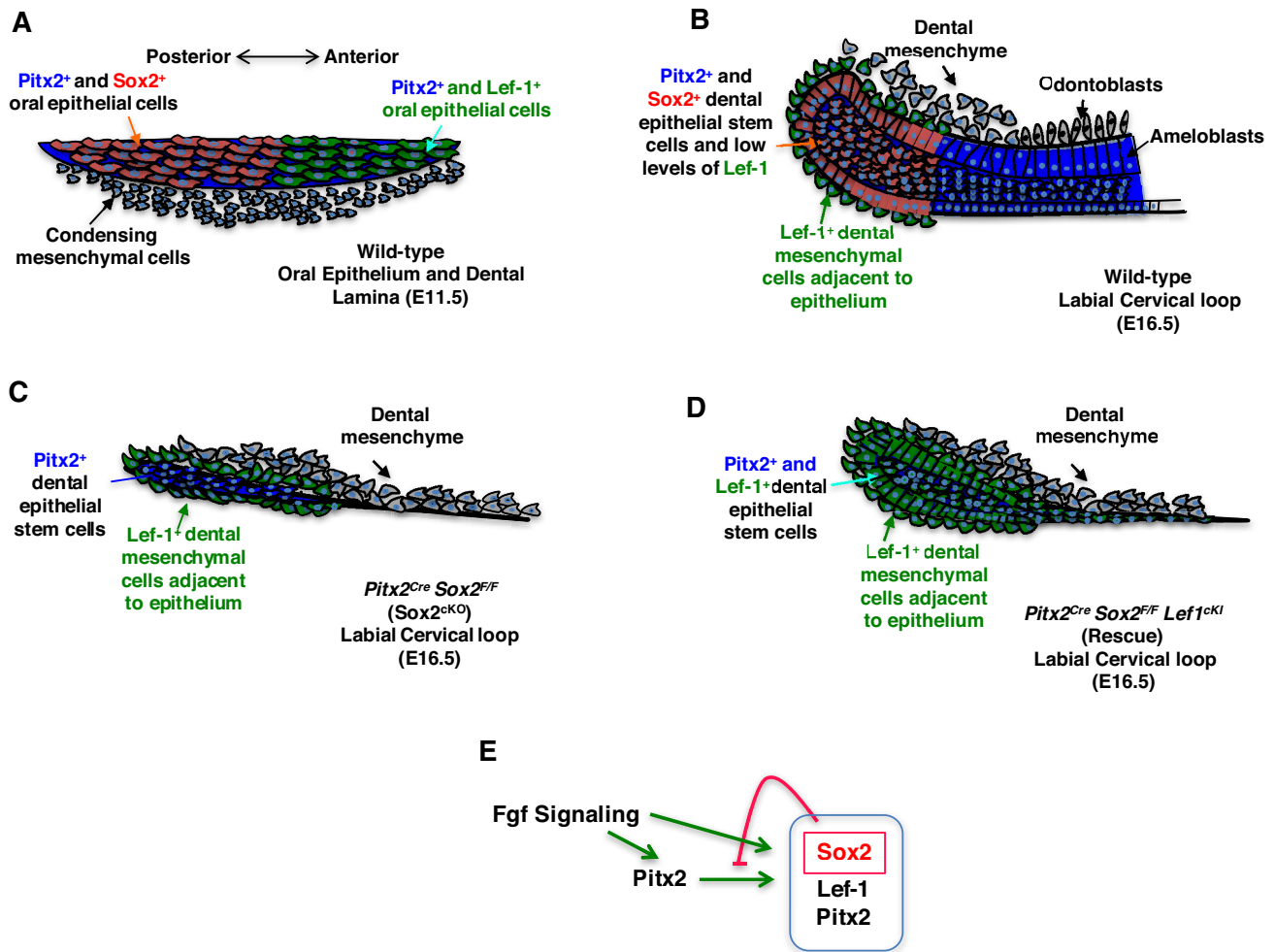


Fig. 7. Model for the roles of *Pitx2*, *Sox2* and *Lef-1* in regulating DESC maintenance and lower incisor development. (A) *Pitx2* (blue) is expressed throughout the dental placode and oral epithelium at E11.5, whereas *Sox2* (red) and *Lef-1* (green) expression occurs in separate domains, with *Sox2* posterior to *Lef-1* in the dental placode. (B) *Pitx2* is expressed with *Sox2* in the LI LaCL at E16.5. However, *Pitx2* is also highly expressed in the transient amplifying cells of the lower incisor that give rise to the ameloblasts. *Lef-1* is mostly expressed in the dental mesenchyme adjacent to the dental epithelium at this stage. (C) In the *Pitx2^{Cre}/Sox2^{F/F}* embryos at E16.5, *Pitx2* is present in the LaCL but *Sox2* and *Lef-1* are absent, leading to the failure to maintain the stem cell niche. (D) In the *Pitx2^{Cre}/Sox2^{F/F}/Lef-1^{cKI}* rescue embryos after E14.5, *Pitx2* and *Lef-1* can function to produce dental epithelial stem cells that generate an incisor. (E) It has been shown that Fgf can activate both *Pitx2* and *Sox2* expression in early stages of tooth development. Biochemical assays in this report show that *Pitx2* activates *Sox2*, *Lef-1* and *Pitx2* to maintain their expression. However, *Sox2* directly interacts with *Pitx2* to repress *Pitx2* transcriptional activity and modulates *Sox2*, *Lef-1* and *Pitx2* expression levels to coordinate dental epithelial stem cell renewal, proliferation and differentiation of progenitor cells.

group of progenitor cells that contribute to the rapid growth of the *COEL* incisors. Thus, the quiescent stem cells are partitioned to a new compartment where they give rise to new progenitor cells.

The upper incisor in *Sox2^{cKO}* embryos also failed to develop normally and at P0 only a remnant remained of the tooth germ. The growth and eruption rate of the upper incisor is slower than that of the lower incisor, which might be due to fewer progenitor cells in the smaller tooth germ of the upper incisor. We speculate that the less severe phenotype of the upper incisor in the *Sox2^{cKO}* embryos might be due to the reduced number of *Sox2⁺* cells regulating its growth. Interestingly, *Lef-1* overexpression greatly increased the growth of the upper incisor.

We found that *Lef-1* overexpression rescues tooth arrest in *Sox2^{cKO}* embryos by enhancing DESC self-renewal and maintenance, further verifying the role of *Lef-1* in stem cell maintenance. In these rescue mice, we found amelogenin aberrantly expressed in the lingual epithelial cell layer. Normally, epithelial stem cells differentiate into ameloblast cells only on the labial side, where they express

amelogenin and secrete the organic matrices of enamel (Thesleff and Tummers, 2009). This complete switch of amelogenin expression to the lingual epithelial cells is similar to other mouse models. Misregulation of BMP signal regulators can cause ameloblast differentiation defects. For example, overexpression of *noggin* or *follistatin* using the *K14* (*Krt14*) promoter disrupts ameloblast differentiation on the labial side of the incisor whereas lack of *follistatin* causes both sides of the incisor to develop functional ameloblasts that secrete enamel (Plikus et al., 2005; Wang et al., 2007, 2004). Ectopic fibroblast growth factor expression in the lingual side of incisors resulting from ablation of sprouty genes leads to ectopic deposition of enamel on the lingual side (Klein et al., 2008, 2006). Although *COEL* embryos do not display this effect, the lack of *Sox2* expression in the incisor tooth germ appears to regulate other factors that might interact with *Lef-1* to regulate amelogenin expression.

Sox2 can have both inductive and repressive transcriptional effects on *Lef-1* promoter activities dependent on other factors to specify

progenitor cell populations during early and late submucosal gland development (Xie et al., 2014). In tooth development, we have identified that the juxtaposed expression of Sox2 and Lef-1 in the dental placode may be coordinated by Pitx2 expression. We have identified a molecular mechanism whereby Pitx2 activates *Pitx2*, *Sox2* and *Lef-1* expression in the dental epithelial stem cells and these activations can be abolished by the Pitx2-Sox2 protein complex. Sox2 interacts with Pitx2 and represses Pitx2 transcriptional activity. The identification of Sox2 protein interactions with Pitx2, resulting in the repression of Pitx2 transcriptional activation of many target genes, provides a model for the role of Sox2 in maintaining the dental stem cells and inhibiting differentiation of these cells. Collectively, our study reveals a Pitx2-Sox2-Lef-1 pathway in regulating DESC maintenance and proliferation and this finding may provide novel molecular approaches for tooth regeneration.

MATERIALS AND METHODS

Mouse lines and embryonic staging

The Program of Animal Resources at the University of Iowa housed mice. Each procedure complied with the guidelines set by the University of Iowa Institutional Animal Care and Use Committee. *Sox2* conditional knockout mice (*Sox2^{Flox/Flox}*) have been previously described (Taranova et al., 2006), and the *ROSA-Cre^{ERT}* [B6.129-Gt(*ROSA*)26Sortm1(*cre/ERT2*)Tyj/J] mice originated from the Jackson Laboratory (stock number 008463). Each of these strains was a generous gift from John Engelhardt (University of Iowa). The *Lef-1* conditional overexpression (*COEL*) mouse line was generated by inserting *Lef-1* downstream of a CAAG promoter and a floxed transcription stop signal. The *Pitx2^{Cre}* mouse has been described previously (Liu et al., 2003). Each mouse line was derived from a C57BL/6 background. The genotyping primers for all the mouse lines are listed in Table S1.

Cloning, transient transfection and luciferase assay

The *Lef-1* 2700 bp (*Lef-1* 2.7) promoter luciferase vector was constructed as previously described (Amen et al., 2007). Sox2 2.0 luciferase reporter was constructed by inserting a ~2.0 kb *Sox2* DNA fragment located in the upstream region of *Sox2* and containing Pitx2-binding sites into the pTK-luc vector. Similarly, ~5.0 kb upstream of the *Pitx2* gene was ligated to pTK-luc to generate the Pitx2 5.0 luciferase reporter. Standard transient transfection by electroporation and luciferase assay were carried out in LS-8 cells (oral epithelial-like cells) according to a previous report (Cao et al., 2013).

Immunohistochemistry, immunofluorescence and histology

The following primary antibodies were used in our study: Sox2 (goat: R&D Systems, AF2018, 1:200; rabbit: Abcam, ab97959, 1:200), GFP (Abcam, ab290, 1:500), Ki67 (Abcam, ab15580, 1:200), Lef-1 (Cell Signaling, #2230, 1:200), cleaved caspase-3 (Cell Signaling, #9661, 1:200) and amelogenin (Santa Cruz, L0506, 1:200). Detailed protocols are provided in the supplementary Materials and Methods.

Quantitative real time PCR gene expression analysis

Total RNAs were extracted from LS-8 cells overexpressing pcDNA 3.1 (empty vector), *Pitx2* or *Sox2* using an RNeasy Mini Kit from Qiagen. Reverse transcription was performed according to the manufacturer's instructions (BIO-RAD iScript Select cDNA Synthesis Kit) using oligo (dT) primers. cDNAs were adjusted to equal levels by PCR amplification with primers to β -actin. Fold change was calculated based on the $2^{-\Delta\Delta CT}$ method. All real-time PCR primer sequences are listed in Table S2.

BrdU labeling and IdU/CldU labeling assay

Two hours prior to sacrifice, pregnant mice were injected with BrdU (10 μ l/g body weight; Invitrogen, 00-0103); rat monoclonal anti-BrdU antibody (Abcam, ab6326, 1:250) was used in this experiment. The IdU/CldU labeling assay was performed according to a previous report with modifications (Tuttle et al., 2010). Detailed protocols are provided in the supplementary Materials and Methods.

Incisor injury and recovery assay

Starting from P21, experimental mice (*Rosa^{CreERT}/Sox2^{F/F}*) and control mice (*Sox2^{F/F}*) were fed with 130 μ g/g bodyweight tamoxifen (Sigma, 75648) daily for a week using a gavage needle. After 8 days of tamoxifen treatment (P29), the left lower incisor of the mouse was clipped and its length was recorded using a caliper. Tamoxifen was administered daily for another three doses (P31, P32 and P34), and the animals were sacrificed at P34. The growth rate was analyzed by daily length increase of the injured incisor [$\text{growth rate} = (\text{length}_{P34} - \text{length}_{P29}) / 5 \text{ days}$]. The relative growth rate was calculated by normalizing the growth rate of injured incisor of experimental mice to control mice.

Chromatin immunoprecipitation assay (ChIP)

The procedure for the ChIP assay has been described previously (Wang et al., 2013). Briefly, the ChIP Assay Kit (Zymo Research, Zymo-Spin ChIP Kit, D5210) was used with a modified protocol. LS-8 cells were seeded in T-75 flasks in DMEM supplemented with 10% fetal bovine serum and 1% penicillin/streptomycin (Life Technology) and fed 24 h prior to the experiment. On the day of the experiment, the adherent cells were harvested and collected in a 1.5 ml tube. The cells were washed twice in cold PBS solution and crosslinked (1% formaldehyde, room temp, 7 min). After crosslinking, cells were subjected to three rounds of sonication (6 s duration, 25% of maximum amplitude), causing lysis and the shearing of genomic DNA in fragments of approximately 200–1000 bp. DNA/protein complexes were immunoprecipitated with 5 μ g Pitx2 antibody (Pitx2 antibody, Capra Sciences, PA-1023) or Sox2 antibody (R&D Systems, AF2018). The same amount of normal rabbit IgG was used to replace the specific antibody to assess the nonspecific immunoprecipitation of the chromatin. All the primer sequences used in this assay are list in Table S2. Three parallel qPCRs were performed using ChIP products. Relative enrichment was calculated using the $2^{-\Delta\Delta CT}$ method. All the PCR products were visualized on a 1.5% agarose gel to check the size and their identities were confirmed by sequencing.

GST pull-down assays

GST pull-down assays were carried out as previously described (Wang et al., 2013). Briefly, GST-Sox2 full-length and truncated fusion proteins were isolated, purified and suspended in binding buffer (20 mM HEPES buffer, pH 7.5, 5% glycerol, 50 mM NaCl, 1 mM EDTA, 1 mM DTT, with 1% milk and 400 μ g/ml ethidium bromide). Bacterially overexpressed and purified Pitx2A protein (2 μ g) was added to 10 μ g immobilized GST fusion protein in a total volume of 100 μ l and incubated for 30 min at 4°C. The beads were pelleted and washed five times with binding buffer. The bound proteins were boiled in SDS loading buffer for 5 min to elute protein from beads. The boiled samples were run on a 12% SDS-PAGE gel. Samples were transferred to a PVDF membrane, immunoblotted and visualized using Pitx2 antibody (Capra Sciences, PA-1023; 1:1000) and ECL reagents (GE HealthCare).

Immunoprecipitation assay

ET16 cells (a gift from Dr Malcolm Snead, University of Southern California) were fed 24 h before the experiment and grown to 90% confluence in two T-175 flasks. Cells were collected and washed twice in ice-cold PBS, and lysed using 5 \times lysis buffer (Promega) in the presence of saturated phenylmethane sulfonyl fluoride (Sigma, P7626). Lysates were repeatedly passed through a 27-gauge needle to disrupt cells. The lysates were then incubated on ice for 30 min and centrifuged at 10,000 *g* for 10 min at 4°C. An aliquot of the supernatant was saved for input. The rest of the supernatant was transferred to a new tube and pre-cleared using the mouse ExactaCruz F IP matrix (ExactaCruz F, Santa Cruz Biotechnology) for 30 min at 4°C. An IP antibody-IP matrix complex was prepared according to the manufacturer's instructions using Pitx2 antibody (Capra Sciences, PA-1023) or rabbit IgG. The IP antibody-IP matrix complex was incubated with pre-cleared cell lysate overnight at 4°C. After incubation, samples were centrifuged to pellet the IP matrix and followed by washing three times with cold PBS and re-suspended in 15 μ l ddH₂O. Samples then were boiled and immunoblotted using anti-Sox2 antibody (Abcam, ab97959).

In situ hybridization

Formalin-fixed paraffin-embedded tissue sections were used for *in situ* hybridization. Tissue samples were prepared following a typical paraffin-embedding process. Frontal sections were cut into segments of 8 μ m, and subsequently prepared according to the standard *in situ* hybridization method described in Gregorieff's protocol (Gregorieff and Clevers, 2015). The digoxigenin-labeled probe was made using a DIG RNA Labeling Kit (Roche # 11175025910). Primers used for the Pitx2 probe were: Pitx2c-F: ACCAACCTACGGAAGCCCGAGT; Pitx2c-T7-R: TAATACGACTACTATAGTCGACTGCATACTGGCAAGCACTCA.

TUNEL assay

Paraffin sections were cut (7 mm) and rehydrated with sequential concentrations of alcohol. The TUNEL assay was carried out using the DeadEnd Fluorometric TUNEL System (Promega, G3250) according to the manufacturer's protocol.

Imaging and microcomputed tomography (μ CT)

Mouse skulls from three experimental and control animals were scanned with a Siemens Inveon Micro-CT/PET scanner using 60 kVp and 500 mA with a voxel size of 30 μ m. Reconstructed images were imported using Osirx DICOM software.

3D reconstruction of the labial cervical loops

Three-dimensional (3D) reconstructions of the labial cervical loop (LaCL) in P2 *Lef-1^{cKI}* and *COEL* mice were made from serial sagittal sections (7.0 μ m). The labial epithelial tissues were manually traced on consecutive sections and automatically aligned using the StackReg plugin for ImageJ. The final 3D reconstructions were rendered using Imaris software from Bitplane AG.

Statistical analysis

For each condition, at least three experiments were performed and the results are presented as mean \pm s.e.m. The differences between two groups were analyzed using an independent, two-tailed *t*-test.

Acknowledgements

Carver Trust Foundation funded the microCT scanner and the image analysis work station. We thank Tom Moninger for help with 3D reconstruction of the incisors. We thank Julie Mayo and Bridget Samuels for critical reading of the manuscript. We thank Drs Hank Qi, Andrew Russo, Martine Dunnwald, Andrew Lidral, Robert Cornell and Liu Hong for reagents, helpful comments and ideas, and all of the members of the Amendt laboratory for their help and comments.

Competing interests

The authors declare no competing or financial interests.

Author contributions

Z.S. designed and performed experiments, analyzed data, wrote the manuscript; W.Y., M.S., S.E., T.S., H.L., L.Z., M.M., T.L., N.E.H., L.R., T.N., designed and performed experiments and analyzed data; M.S.N., K.S., M.J.G., F.M., O.D.K., Y.C., A.D., J.F.E., Z.C. provided reagents, manuscript editing, experimental details, and comments; B.A.A. designed experiments, analyzed data, wrote the manuscript.

Funding

This work was supported by funds from the University of Iowa Carver College of Medicine and University of Iowa College of Dentistry; the National Institutes of Health [DE13941 to B.A.A., R37 DE012711 to Y.C.]; and the National Natural Science Foundation of China [81400477 to H.L.]. Deposited in PMC for release after 12 months.

Supplementary information

Supplementary information available online at <http://dev.biologists.org/lookup/doi/10.1242/dev.138883.supplemental>

References

Amen, M., Liu, X., Vadlamudi, U., Elizondo, G., Diamond, E., Engelhardt, J. F. and Amendt, B. A. (2007). PITX2 and β -catenin interactions regulate Lef-1 isoform expression. *Mol. Cell. Biol.* **27**, 7560–7573.

Arnold, K., Sarkar, A., Yram, M. A., Polo, J. M., Bronson, R., Sengupta, S., Seandel, M., Geijsen, N. and Hochedlinger, K. (2011). Sox2(+) adult stem and

progenitor cells are important for tissue regeneration and survival of mice. *Cell Stem Cell* **9**, 317–329.

- Avilion, A. A., Nicolis, S. K., Pevny, L. H., Perez, L., Vivian, N. and Lovell-Badge, R. (2003). Multipotent cell lineages in early mouse development depend on SOX2 function. *Genes Dev.* **17**, 126–140.
- Balaguer, F., Moreira, L., Lozano, J. J., Link, A., Ramirez, G., Shen, Y., Cuatrecasas, M., Arnold, M., Meltzer, S. J., Syngal, S. et al. (2011). Colorectal cancers with microsatellite instability display unique miRNA profiles. *Clin. Cancer Res.* **17**, 6239–6249.
- Biehs, B., Hu, J. K.-H., Strauli, N. B., Sangiorgi, E., Jung, H., Heber, R.-P., Ho, S., Goodwin, A. F., Dasen, J. S., Capecchi, M. R. et al. (2013). BMI1 represses Ink4a/Arf and Hox genes to regulate stem cells in the rodent incisor. *Nat. Cell Biol.* **15**, 846–852.
- Boyer, L. A., Lee, T. I., Cole, M. F., Johnstone, S. E., Levine, S. S., Zucker, J. P., Guenther, M. G., Kumar, R. M., Murray, H. L., Jenner, R. G. et al. (2005). Core transcriptional regulatory circuitry in human embryonic stem cells. *Cell* **122**, 947–956.
- Cao, H., Wang, J., Li, X., Florez, S., Huang, Z., Venugopalan, S. R., Elangovan, S., Skobe, Z., Margolis, H. C., Martin, J. F. et al. (2012). MicroRNAs play a critical role in tooth development. *J. Dent. Res.* **89**, 779–784.
- Cao, H., Jheon, A., Li, X., Sun, Z., Wang, J., Florez, S., Zhang, Z., McManus, M. T., Klein, O. D. and Amendt, B. A. (2013). The Pitx2:miR-200c/141:noggin pathway regulates Bmp signaling and ameloblast differentiation. *Development* **140**, 3348–3359.
- Clavel, C., Grisanti, L., Zemla, R., Rezza, A., Barros, R., Sennett, R., Mazloom, A. R., Chung, C.-Y., Cai, X., Cai, C.-L. et al. (2012). Sox2 in the dermal papilla niche controls hair growth by fine-tuning BMP signaling in differentiating hair shaft progenitors. *Dev. Cell* **23**, 981–994.
- Ellis, P., Fagan, B. M., Magness, S. T., Hutton, S., Taranova, O., Hayashi, S., McMahon, A., Rao, M. and Pevny, L. (2004). SOX2, a persistent marker for multipotential neural stem cells derived from embryonic stem cells, the embryo or the adult. *Dev. Neurosci.* **26**, 148–165.
- Gregorieff, A. and Clevers, H. (2015). In situ hybridization to identify gut stem cells. *Curr. Protoc. Stem Cell Biol.* **34**, 1–11.
- Huang, C. and Qin, D. (2010). Role of Lef1 in sustaining self-renewal in mouse embryonic stem cells. *J. Genet. Genomics* **37**, 441–449.
- Jayakody, S. A., Andoniadou, C. L., Gaston-Massuet, C., Signore, M., Cariboni, A., Bouloux, P. M., Le Tissier, P., Pevny, L. H., Dattani, M. T. and Martinez-Barbera, J. P. (2012). SOX2 regulates the hypothalamic-pituitary axis at multiple levels. *J. Clin. Invest.* **122**, 3635–3646.
- Juuri, E., Saito, K., Ahtainen, L., Seidel, K., Tummars, M., Hochedlinger, K., Klein, O. D., Thesleff, I. and Michon, F. (2012). Sox2+ stem cells contribute to all epithelial lineages of the tooth via Sfrp5+ progenitors. *Dev. Cell* **23**, 317–328.
- Juuri, E., Jussila, M., Seidel, K., Holmes, S., Wu, P., Richman, J., Heikinheimo, K., Chuong, C.-M., Arnold, K., Hochedlinger, K. et al. (2013). Sox2 marks epithelial competence to generate teeth in mammals and reptiles. *Development* **140**, 1424–1432.
- Kaukua, N., Shahidi, M. K., Konstantinidou, C., Dyachuk, V., Kauka, M., Furlan, A., An, Z., Wang, L., Hultman, I., Ahrlund-Richter, L. et al. (2014). Glial origin of mesenchymal stem cells in a tooth model system. *Nature* **513**, 551–554.
- Klein, O. D., Minowada, G., Peterkova, R., Kangas, A., Yu, B. D., Lesot, H., Peterka, M., Jernvall, J. and Martin, G. R. (2006). Sprouty genes control diastema tooth development via bidirectional antagonism of epithelial-mesenchymal FGF signaling. *Dev. Cell* **11**, 181–190.
- Klein, O. D., Lyons, D. B., Balooch, G., Marshall, G. W., Basson, M. A., Peterka, M., Boran, T., Peterkova, R. and Martin, G. R. (2008). An FGF signaling loop sustains the generation of differentiated progeny from stem cells in mouse incisors. *Development* **135**, 377–385.
- Kratochwil, K., Dull, M., Farinas, I., Galceran, J. and Grosschedl, R. (1996). Lef1 expression is activated by BMP-4 and regulates inductive tissue interactions in tooth and hair development. *Genes Dev.* **10**, 1382–1394.
- Kratochwil, K., Galceran, J., Tontsch, S., Roth, W. and Grosschedl, R. (2002). FGF4, a direct target of LEF1 and Wnt signaling, can rescue the arrest of tooth organogenesis in Lef1(-/-) mice. *Genes Dev.* **16**, 3173–3185.
- Lane, S. W., Williams, D. A. and Watt, F. M. (2014). Modulating the stem cell niche for tissue regeneration. *Nat. Biotechnol.* **32**, 795–803.
- Li, X., Venugopalan, S. R., Cao, H., Pinho, F. O., Paine, M. L., Snead, M. L., Semina, E. V. and Amendt, B. A. (2013). A model for the molecular underpinnings of tooth defects in Axenfeld-Rieger syndrome. *Hum. Mol. Genet.* **23**, 194–208.
- Li, J., Feng, J., Liu, Y., Ho, T.-V., Grimes, W., Ho, H. A., Park, S., Wang, S. and Chai, Y. (2015). BMP-SHH signaling network controls epithelial stem cell fate via regulation of its niche in the developing tooth. *Dev. Cell* **33**, 125–135.
- Liu, W., Selever, J., Lu, M.-F. and Martin, J. F. (2003). Genetic dissection of Pitx2 in craniofacial development uncovers new functions in branchial arch morphogenesis, late aspects of tooth morphogenesis and cell migration. *Development* **130**, 6375–6385.
- Lowry, W. E., Blanpain, C., Nowak, J. A., Guasch, G., Lewis, L. and Fuchs, E. (2005). Defining the impact of beta-catenin/Tcf transactivation on epithelial stem cells. *Genes Dev.* **19**, 1596–1611.

- Lu, M.-F., Pressman, C., Dyer, R., Johnson, R. L. and Martin, J. F. (1999). Function of Rieger syndrome gene in left-right asymmetry and craniofacial development. *Nature* **401**, 276–278.
- Moore, K. E., Mills, J. F. and Thornton, M. M. (2006). Alternative sources of adult stem cells: a possible solution to the embryonic stem cell debate. *Gen. Med.* **3**, 161–168.
- Petersson, M., Brylka, H., Kraus, A., John, S., Rappl, G., Schettina, P. and Niemann, C. (2011). TCF/Lef1 activity controls establishment of diverse stem and progenitor cell compartments in mouse epidermis. *EMBO J.* **30**, 3004–3018.
- Plikus, M. V., Zeichner-David, M., Mayer, J.-A., Reyna, J., Bringas, P., Thewissen, J. G. M., Snead, M. L., Chai, Y. and Chuong, C.-M. (2005). Morphoregulation of teeth: modulating the number, size, shape and differentiation by tuning Bmp activity. *Evol. Dev.* **7**, 440–457.
- Que, J., Okubo, T., Goldenring, J. R., Nam, K.-T., Kurotani, R., Morrisey, E. E., Taranova, O., Pevny, L. H. and Hogan, B. L. M. (2007). Multiple dose-dependent roles for Sox2 in the patterning and differentiation of anterior foregut endoderm. *Development* **134**, 2521–2531.
- Sasaki, T., Ito, Y., Xu, X., Han, J., Bringas, P., Maeda, T., Slavkin, H. C., Grosschedl, R. and Chai, Y. (2005). LEF1 is a critical epithelial survival factor during tooth morphogenesis. *Dev. Biol.* **278**, 130–143.
- Smith, C. E. and Warshawsky, H. (1975). Cellular renewal in the enamel organ and the odontoblast layer of the rat incisor as followed by radioautography using 3H-thymidine. *Anat. Rec.* **183**, 523–561.
- Smith, M. M., Fraser, G. J. and Mitsiadis, T. A. (2009). Dental lamina as source of odontogenic stem cells: evolutionary origins and developmental control of tooth generation in gnathostomes. *J. Exp. Zool. B Mol. Dev. Evol.* **312B**, 260–280.
- Spradling, A., Drummond-Barbosa, D. and Kai, T. (2001). Stem cells find their niche. *Nature* **414**, 98–104.
- Takahashi, K. and Yamanaka, S. (2006). Induction of pluripotent stem cells from mouse embryonic and adult fibroblast cultures by defined factors. *Cell* **126**, 663–676.
- Taranova, O. V., Magness, S. T., Fagan, B. M., Wu, Y., Surzenko, N., Hutton, S. R. and Pevny, L. H. (2006). SOX2 is a dose-dependent regulator of retinal neural progenitor competence. *Genes Dev.* **20**, 1187–1202.
- Thesleff, I. and Tummers, M. (2009). Tooth organogenesis and regeneration. In *StemBook*. Cambridge (MA, USA): Harvard Stem Cell Institute.
- Tuttle, A. H., Rankin, M. M., Teta, M., Sartori, D. J., Stein, G. M., Kim, G. J., Virgilio, C., Granger, A., Zhou, D., Long, S. H. et al. (2010). Immunofluorescent detection of two thymidine analogues (CldU and IdU) in primary tissue. *J. Vis. Exp.* **46**, 2166.
- Vadlamudi, U., Espinoza, H. M., Ganga, M., Martin, D. M., Liu, X., Engelhardt, J. F. and Amendt, B. A. (2005). PITX2, β -catenin, and LEF-1 interact to synergistically regulate the LEF-1 promoter. *J. Cell Sci.* **118**, 1129–1137.
- van Genderen, C., Okamura, R. M., Farinas, I., Quo, R. G., Parslow, T. G., Bruhn, L. and Grosschedl, R. (1994). Development of several organs that require inductive epithelial-mesenchymal interactions is impaired in LEF-1-deficient mice. *Genes Dev.* **8**, 2691–2703.
- Wang, X.-P., Suomalainen, M., Jorgez, C. J., Matzuk, M. M., Werner, S. and Thesleff, I. (2004). Follistatin regulates enamel patterning in mouse incisors by asymmetrically inhibiting BMP signaling and ameloblast differentiation. *Dev. Cell* **7**, 719–730.
- Wang, X.-P., Suomalainen, M., Felszeghy, S., Zelarayan, L. C., Alonso, M. T., Plikus, M. V., Maas, R. L., Chuong, C.-M., Schimmang, T. and Thesleff, I. (2007). An integrated gene regulatory network controls stem cell proliferation in teeth. *PLoS Biol.* **5**, e159.
- Wang, J., Saadi, I., Wang, J., Engel, J. J., Kaburas, A., Russo, A. F. and Amendt, B. A. (2013). PIAS1 and PIASy differentially regulate PITX2 transcriptional activities. *J. Biol. Chem.* **288**, 12580–12595.
- Xie, J., Ameres, S. L., Friedline, R., Hung, J.-H., Zhang, Y., Xie, Q., Zhong, L., Su, Q., He, R., Li, M. et al. (2012). Long-term, efficient inhibition of microRNA function in mice using rAAV vectors. *Nat. Methods* **9**, 403–409.
- Xie, W., Lynch, T. J., Liu, X., Tyler, S. R., Yu, S., Zhou, X., Luo, M., Kusner, D. M., Sun, X., Yi, Y. et al. (2014). Sox2 modulates Lef-1 expression during airway submucosal gland development. *Am. J. Physiol. Lung Cell. Mol. Physiol.* **306**, L645–L660.
- Zhang, L., Yuan, G., Liu, H., Lin, H., Wan, C. and Chen, Z. (2012). Expression pattern of Sox2 during mouse tooth development. *Gene Expr. Patterns* **12**, 273–281.
- Zhao, H., Feng, J., Seidel, K., Shi, S., Klein, O., Sharpe, P. and Chai, Y. (2014). Secretion of shh by a neurovascular bundle niche supports mesenchymal stem cell homeostasis in the adult mouse incisor. *Cell Stem Cell* **14**, 160–173.

Supplemental Experimental Procedures

Immunohistochemistry, Immunofluorescence and Histology

Mouse embryos or heads were dissected in a cold PBS solution, and fixed from one to four hours in 4% paraformaldehyde while protected from light. After fixation, the tissues were dehydrated through an ethanol gradient (70% for over an hour, 80% for over an hour, 95% for over an hour, and 100% overnight), perforated with xylene, embedded in paraffin and with a microtome, sectioned into 7µm thick segments. Tissue morphology was examined by Hematoxylin and Eosin staining (Cao et al., 2013). Sections used for analysis by immunofluorescence and immunohistochemistry were subjected to antigen retrieval by raising them to 95°C in a citrate buffer (10mM, pH 6.0) for 20 minutes. Blocking was performed by incubating the sections with 20% donkey serum in PBS-triton at room temperature for 30 minutes. Primary antibodies against Sox2 (Goat, R&D Systems, AF2018 1:200; Rabbit Abcam, ab97959, 1:200), GFP (Abcam ab290, 1:500), Ki67 (Abcam, ab15580, 1:200), Lef-1 (Cell signaling #2230, 1:200), , Cleaved caspase-3 (Cell signaling, #9661, 1:200) and amelogenin (Santa Cruz, L0506, 1:200) were then added to the sections. Incubation with primary antibody occurred overnight at 4°C. The slides were treated with FITC (Alexa-488)- or Texas Red (Alexa-555)-conjugated secondary antibody for 30 minutes at room temperature for detection (Invitrogen, 1:400). Nuclear counterstaining was performed using DAPI-containing mounting solution. For immunohistochemistry, standard protocols were followed according to the manufacturer's manual (Millipore, IHC select HRP/DAB, DAB150). Images were captured by a Nikon eclipse 80i fluorescence microscope or Zeiss 700 confocal microscope.

BrdU labeling

Two hours prior to sacrifice, pregnant mice were injected with BrdU (10µl/g body weight, Invitrogen, 00-0103), and the embryos were collected and processed as previously described in the immunofluorescence assay. Sections were mounted and rehydrated through a reverse ethanol gradient, and to compensate for endogenous peroxidase activity, immersed in 3% hydrogen peroxide. Antigen retrieval was performed by immersing sections in 10 mM sodium citrate solution for 20 min at a slow boiling state. Sections were perforated by a 30 minute incubation in 2 M HCl, followed by a neutralization step (10 minutes in 0.1M Na₂B₄O₇). Sections were

subsequently blocked for 1 hr in 10% donkey serum, and labeled with anti-BrdU antibody (Abcam ab6326, 1:250). Next, standard immunohistochemistry staining was carried out as described above for the immunohistochemistry assays. Experimental and control sections were processed together on the same slide for identical time periods.

IdU/CldU labeling assay

Standard immunofluorescent detection of IdU/CldU was performed according to previous report with modifications (Tuttle et al., 2010). 24 hours prior to harvesting E 15.5 mouse embryos, pregnant female mice were intraperitoneally injected with 100 µg per gram of body weight of CldU (Sigma, C6891). One hour before harvesting the embryos, the pregnant female mice were again injected with 100 µg per gram of body weight of IdU (Sigma, I7125). Mouse embryos were then harvested and embedded in paraffin. The blocks were sectioned and subjected to antigen retrieval by boiling in citrate buffer (10mM, pH 6.0) for 20 min. Sections were then perforated by incubating in 1.5 M HCl at 37°C for 30 minute, followed by a neutralization step (10 minutes 0.1M Na₂B₄O₇ at room temperature). Next, sections were blocked in 10% donkey serum diluted in PBST (PBS with 0.05% Triton-100) for one hour at room temperature. Slides were treated with a primary antibody, mouse anti-BrdU/IdU (Roche, 11170376001,1:250), overnight at 4°C to detect IdU. Slides then were stringently washed by vigorous agitation in a shaker for 20 min with low-salt TBST buffer (36mM Tris, 50mM NaCl, 0.5% tween-20; pH 8.0) at 37°C, at a speed of 200 rpm. Sections were washed twice with PBST (10 minutes each), and treated with a primary antibody against CldU (anti BrdU/CldU, Accurate chemical, OBT0030, 1:250) for 2hr at room temperature. Slides were washed three times with PBST, treated with a mix of secondary antibodies (Rhodamine-Red donkey anti-rat, Jackson ImmunoResearch, #712-296-153,1:400; Alex Fluor488 donkey anti-mouse IgG, Invitrogen, A21202, 1:400) for half an hour at room temperature, and then washed three times in 1x PBST for 10 minutes. Slides were covered using a mounting solution containing DAPI (Vector lab, H-1200) and prepared for imaging.

Supplemental References

Cao, H., Jheon, A., Li, X., Sun, Z., Wang, J., Florez, S., Zhang, Z., McManus, M.T., Klein, O.D., and Amendt, B.A. (2013). The Pitx2:miR-200c/141:noggin pathway regulates Bmp signaling and ameloblast differentiation. *Development* **140**, 3348-3359.

Tuttle, A.H., Rankin, M.M., Teta, M., Sartori, D.J., Stein, G.M., Kim, G.J., Virgilio, C., Granger, A., Zhou, D., Long, S.H., et al. (2010). Immunofluorescent detection of two thymidine analogues (CldU and IdU) in primary tissue. *J. Vis. Exp.* **46**, 2166.

Table S1: List of the primers for genotyping.

Mouse lines	Genotyping primers
<i>Pitx2^{Cre}</i>	Cre-Forward: GCATTACCGGTCGATGCAACGAGTGATG Cre-Reverse: GAGTGAACGAACCTGGTCGAAATCAGTGC
<i>Krt14^{Cre}</i>	Same as Pitx2-Cre
<i>Shh^{Cre}</i>	Shh-cre Forward: TGCCAGGATCAGGGTTTAAG Shh-cre Reverse: GCTTGCATGATCTCCGGTAT
<i>Rosa26^{CreERT}</i>	Rosa26-Cre Forward: AAAGTCGCTCTGAGTTGTTAT Rosa26-Cre Reverse: CCTGATCCTGGCAATTTTCG
<i>Sox2^{F/F}</i>	Sox2Flox mut F: CAGCAGCCTCTGTTCCACATACAC Sox2Flox mut R: CAACGCATTTTCAGTTCCCCG Sox2Flox WT F: GCTCTGTTATTGGAATCAGGCTGC Sox2Flox WT R: CTGCTCAGGGAAGGAGGGG
<i>Lef-1^{cKI/cKI}</i>	Lef-1cKI mut F: TGAGGCGGAAGTTCTATTCT Lef-1cKI mut R: GGCGGATCACAAGCAATAAT Lef-1cKI WT F: TCCCAAAGTCGCTCTGAGTT Lef-1cKI WT R: GGCGGATCACAAGCAATAAT
<i>Rosa26^{Tomato-GFP}</i>	Tomato-GFP mut F: CTCTGCTGCCTCCTGGCTTCT Tomato-GFP mut R: CGAGGCGGATCACAAGCAATA Tomato-GFP WT F: CTCTGCTGCCTCCTGGCTTCT Tomato-GFP WT R: TCAATGGGCGGGGGTTCGTT

Table S2: Primer list for ChIP assay and Real-time PCR.

Primer name	Forward primer(5'-3')	Reverse primer(5'-3')
Pitx2 ChIP 1	AGGGCTGGGAGAAAGAAGAG	ATCTGGCGGAGAATAGTTGG
Pitx2 ChIP 2	GAGCTTCTTTCCGTTGATGC	TTCCCTACTCCACCAACCTG
Pitx2 ChIP control	GGCAGAGTTGGGGTAGATGA	CCCCGTCTAAGTTTCCTTCC
Sox2 ChIP	GCTCAACCTTTGCTCTGGTC	TAGTCCACCCCTCTCACTGC
Sox2 ChIP control	GCCTGGCTCCAATGTAATGT	CATTCCGAGGAAGAGCAGAC
Lef-1	TCACTGTCAGGCGACACTTC	ATGAGGTCTTTTGGGCTCCT
Sox2	ATGCACAACCTCGGAGATCAG	TGAGCGTCTTGGTTTTCCG
Pitx2	CTGGAAGCCACTTTCCAGAG	AAGCCATTCTTGACAGCTC
β - Actin	GCCTTCCTTCTTGGGTATG	ACCACCAGACAGCACTGTG

Supplementary Figures

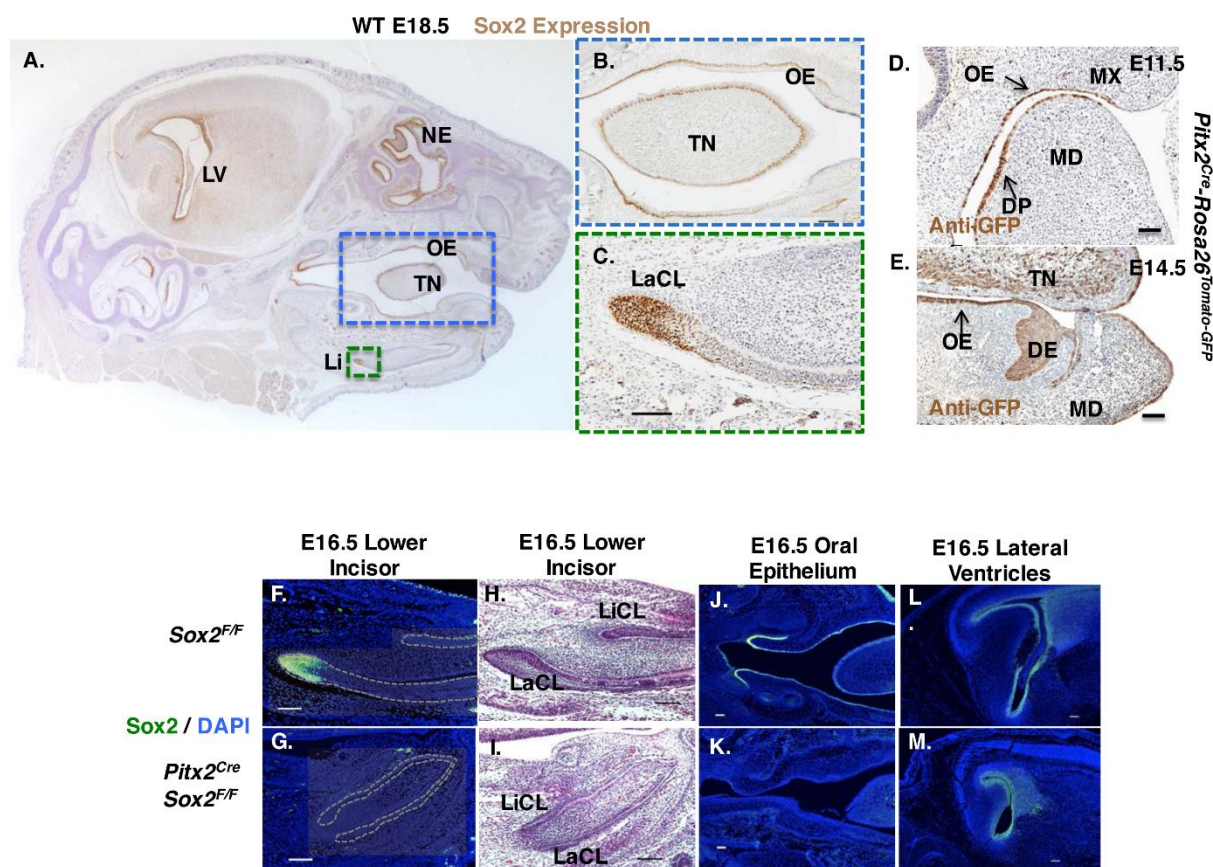


Figure S1. *Sox2* expression in the dental epithelial stem cell niche (LaCL) and loss of *Sox2* expression in the dental and oral epithelia in the *Pitx2^{Cre}/Sox2^{F/F}* (*Sox2^{cKO}*) embryos. **A)** Immunohistochemistry staining of sagittal sections from a WT E18.5 head using a *Sox2* antibody reveals that *Sox2* is expressed in the lateral ventricle (LV), nasal epithelium (NE), tongue epithelium (TN), oral epithelium (OE) and lower incisor (Li). Nuclei are counterstained with hematoxylin. **B, C)** Magnified views of the blue and green-boxed regions, respectively in (A). **B)** *Sox2* expression in the OE and TN, **C)** *Sox2* expression is localized in the labial cervical loop (LaCL) of the mouse lower incisor. **D, E)** Expression of *Pitx2^{Cre}* at E11.5 and E14.5, respectively (*Pitx2^{Cre} X Rosa26^{tomato-GFP}*). **F-M)** Immunofluorescence staining of *Sox2* in the lower incisor LaCL, oral epithelium and lateral ventricles of *Sox2^{F/F}* (Control) and *Pitx2^{Cre}/Sox2^{F/F}* (*Sox2^{cKO}*) mice verified the specificity of the deletion of *Sox2* by the *Pitx2^{Cre}*. Nuclei are counterstained with DAPI. MD, mandible; MX, maxilla; DE, dental epithelium; DP, dental placode, Scale bars, 100 μ m.

In the panel L, the panel "." Should on the right side of "L"

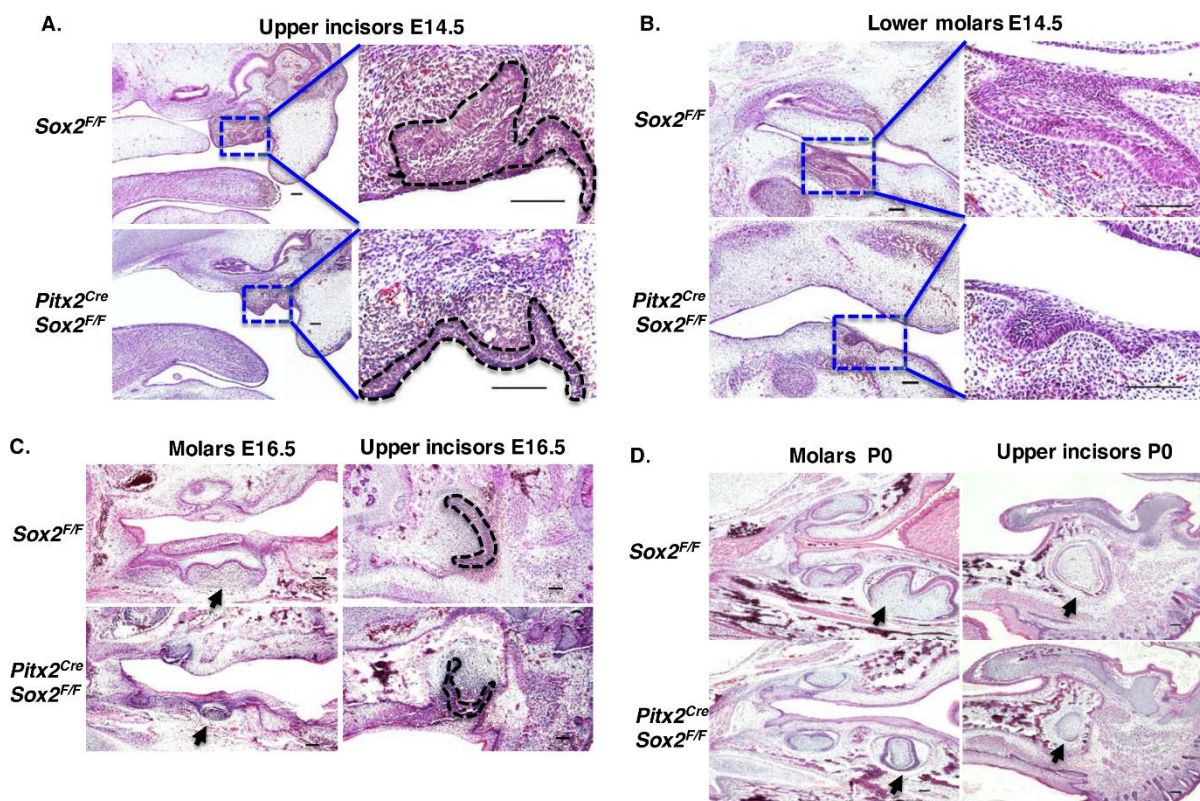


Figure S2. Molar and upper incisor development is impaired in $Sox2^{cKO}$ embryos.

A) H&E staining of sagittal section E14.5 upper incisors (UI) shows that $Sox2^{cKO}$ UI are smaller with incomplete invagination compared with control ($Sox2^{F/F}$). Boxed areas are shown as magnified images on the right (Dotted lines indicate tooth buds). **B)** E14.5 lower molars (LMs) (sagittal section) stained by H&E indicate $Sox2^{cKO}$ embryos have a smaller LM with incomplete invagination compared to controls. Boxed areas are shown as magnified images on the right. **C)** H&E staining of E16.5 UI and molars show a smaller size and abnormal shape in $Sox2^{cKO}$ embryos compared with controls. Arrows indicate molars and dotted line indicates UI). **D)** P0 molars and upper incisors stained with H&E. $Sox2^{cKO}$ molars are smaller and hypoplastic compared with control molars. Upper incisors are also smaller in $Sox2^{cKO}$ mice. Arrows indicate molars and UI, respectively). Scale bars, 100 μ m.

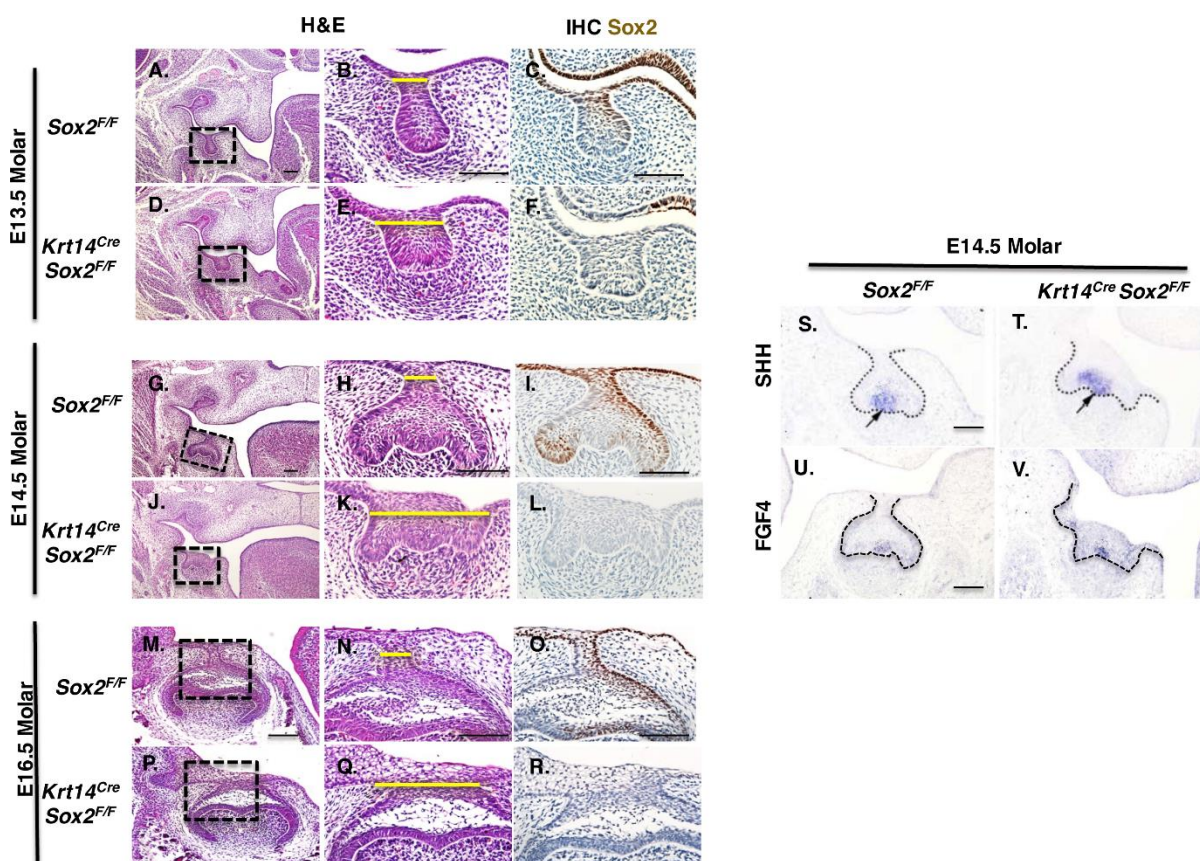


Figure S3. *Sox2* ablation with the *Krt14*^{Cre} causes abnormal molar formation and changes in *Shh* and *Fgf4* expression.

A-F) At E13.5, invagination of the lower molar tooth bud was displaced with a wide dental lamina and tooth bud structure (yellow line) in the *Krt14*^{Cre}/*Sox2*^{F/F} (E, F), compared to controls (B, C). **G-L)** At E14.5, invagination was affected and the dental lamina was significantly larger in *Krt14*^{Cre}/*Sox2*^{F/F} embryos compared to controls. **M-R)** At E15.5, the invagination defect persisted with abnormal formation of the molar in the *Krt14*^{Cre}/*Sox2*^{F/F} embryos. Interestingly, in the incisors *Sox2* was asymmetrically expressed (C, I, O). **S, T)** *Shh* transcripts were detected in the *Sox2*^{F/F} enamel knot structure of the E14.5 lower molar, however the *Shh* expression domain was expanded in the *Krt14*^{Cre}/*Sox2*^{F/F} lower molar, as the *Shh* domain moved towards the presumptive *Sox2* region. **U, V)** *Fgf4* expression (transcripts) was slightly increased in the *Krt14*^{Cre}/*Sox2*^{F/F} lower molars.

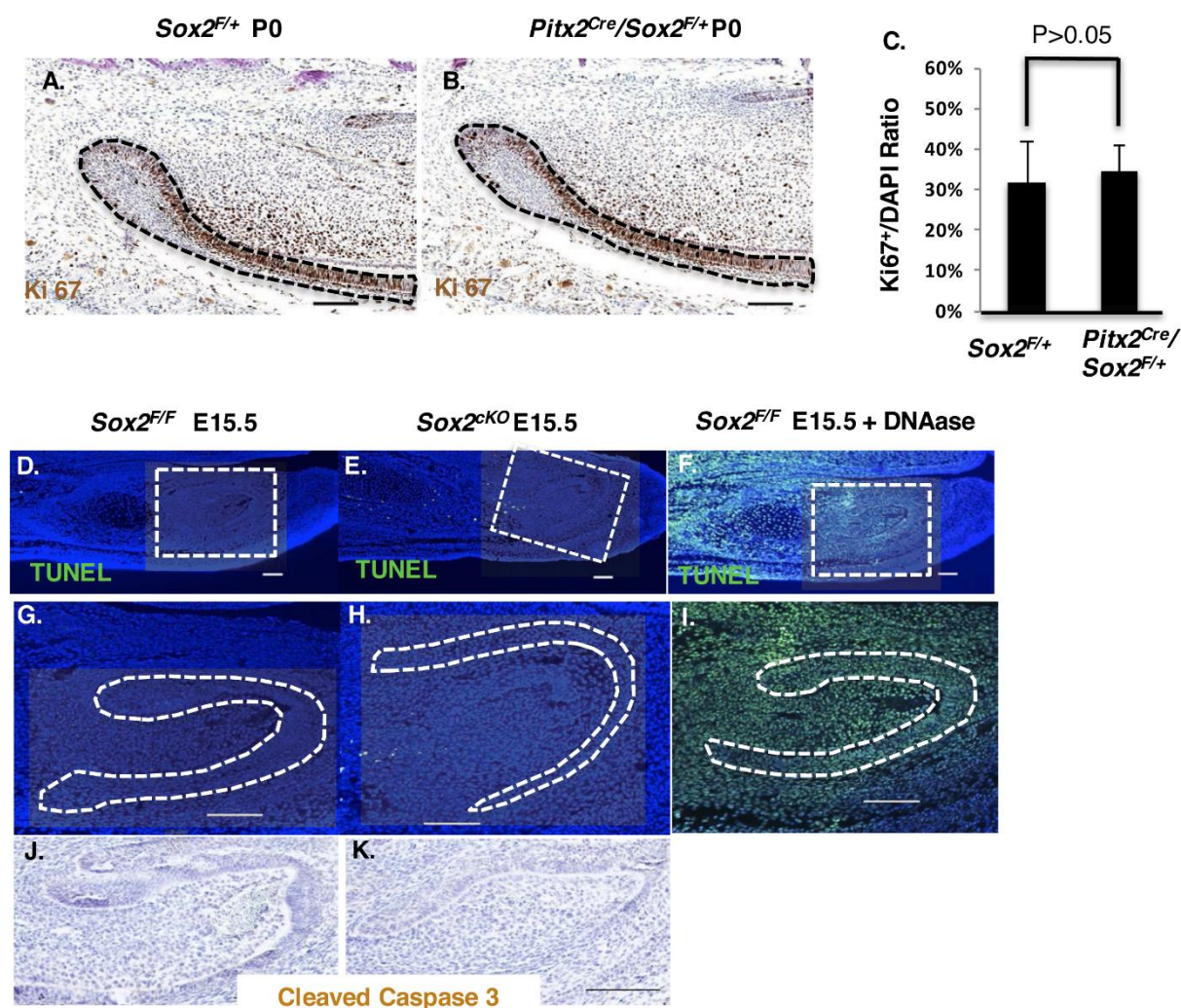


Figure S4. Loss of dental epithelial stem cells in *Sox2^{cKO}* embryos does not involve increased apoptosis.

A-B) Control experiments show that proliferation of the dental epithelial cells in the LaCL was not affected in the P0 *Sox2^{F/+}* or *Pitx2^{Cre}/Sox2^{F/+}* embryos. **C)** Quantitation of the Ki67 stained cells in the *Pitx2^{Cre}/Sox2^{F/+}* embryos and controls shows no difference in proliferation between groups. **D-I)** TUNEL staining in E15.5 (sagittal section) mouse lower incisors reveals no changes in apoptosis in *Sox2^{cKO}* embryos. Magnified view of boxed regions in D, E and F are shown in G, H and I respectively. No apparent apoptosis signal was detected in control or *Sox2^{cKO}* incisors. (F, I) are positive controls for TUNEL staining. N=3. Nuclei are counterstained with DAPI **J, K)** Immunohistochemistry staining of the early apoptosis marker cleaved Caspase 3 in sagittal sections of E15.5 mouse incisors showing no detectable level of apoptosis in control and *Sox2^{cKO}* incisors, N=3. Nuclei are counterstained with hematoxylin. Scale bars, 100 μ m.

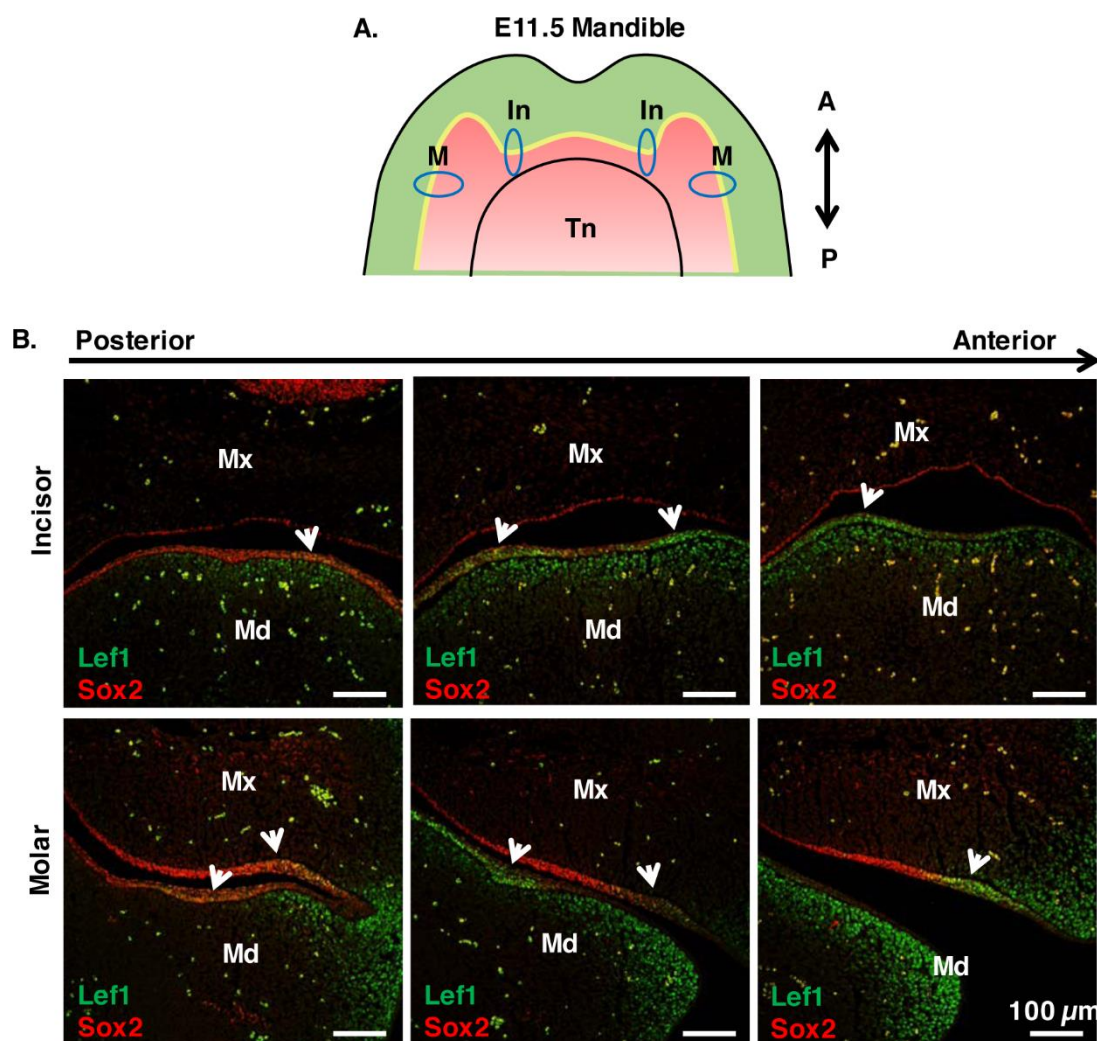


Figure S5. Sox2 expression is posterior to Lef-1 in developing incisors and molars.

A) Schematic of the murine E11.5 mandible showing Sox2 expression in red and Lef-1 expression in green. The locations of the incisors (In) and molars (M) are shown by blue circles (A, anterior; P, posterior; Tn tongue). **B)** Merged photos of Sox2 and Lef-1 immunofluorescence staining in E11.5 WT embryos from posterior to anterior showing the juxtaped expression domains of these two factors. Arrows denote the dental placodes.

Mx, maxilla; Md, mandible. Scale bars, 100μm.

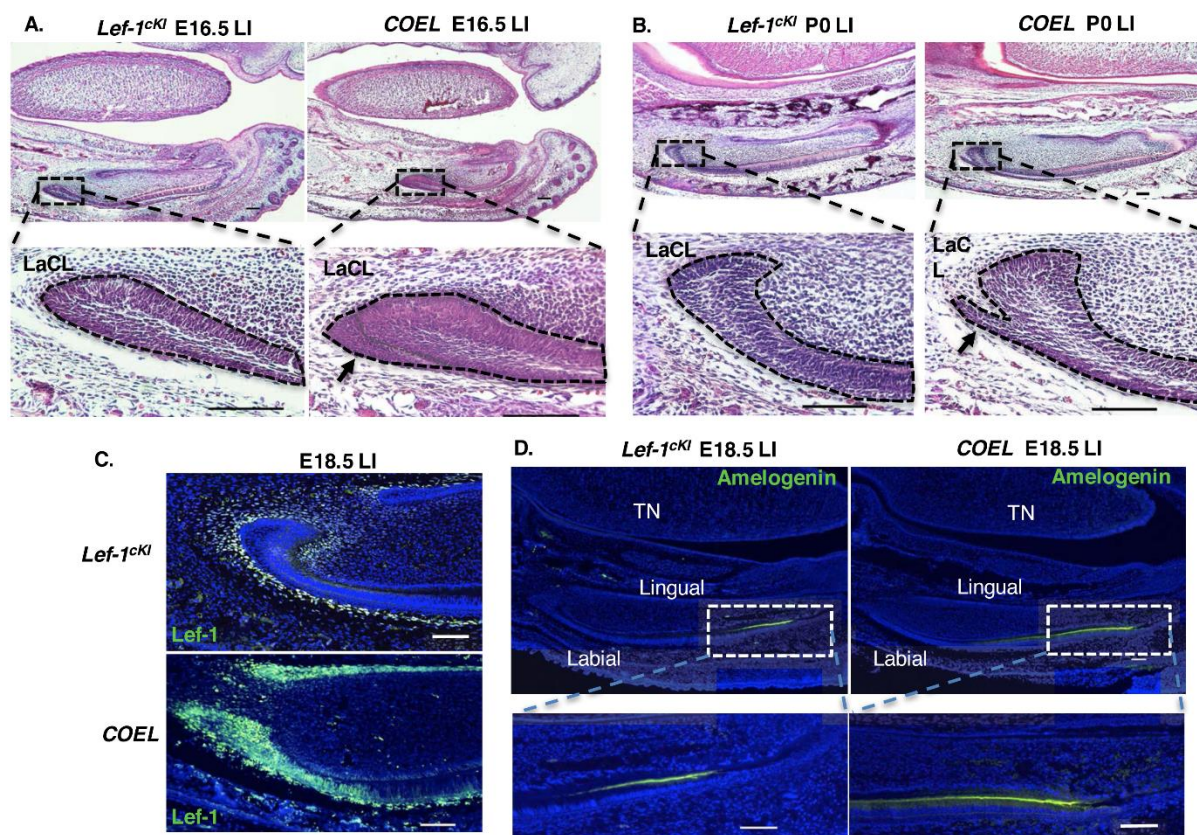


Figure S6. Overexpression of *Lef-1* in dental and oral epithelia creates a new LaCL stem cell compartment and increased amelogenin expression.

A, B) H&E staining of lower incisors (sagittal sections) shows an enlarged LaCL in E16.5 *COEL* incisors compared to controls (*Lef-1^{CKI}*). The arrow denotes the separation of a new stem cell compartment from the normal cervical loop structure in the *COEL* LI. A newly formed stem cell compartment (arrow) that has branched from the LaCL was observed in P0 *COEL* incisors (N=3). **C)** Lef-1 immunofluorescence staining in E18.5 lower incisors shows Lef-1 was overexpressed in the LaCL and LiCL of the *COEL* embryos. **D)** Amelogenin immunofluorescence staining in E18.5 lower incisors indicates increased amelogenin expression in *COEL* incisors compared to control incisors. Nuclei are counterstained with DAPI. Tn, tongue. Scale bars, 100µm.

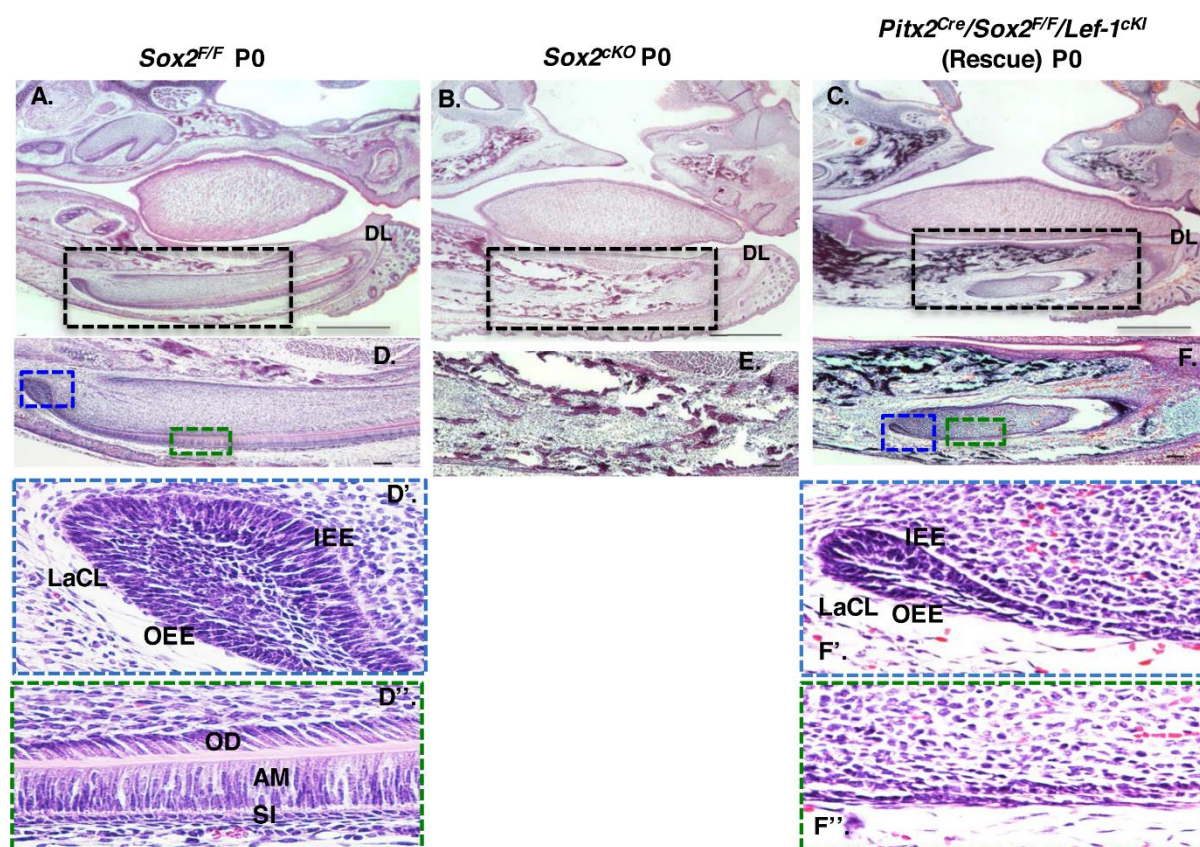


Figure S7. *Lef-1* overexpression rescues lower incisor development in *Sox2^{cKO}* embryos.

A-C) H&E staining (sagittal sections) of P0 *Sox2^{F/F}* (control), *Sox2^{cKO}* and *Pitx2^{Cre}/Sox2^{F/F}/Lef-1^{cKI}* (*Lef-1* rescue *Sox2^{cKO}*) embryos. D-F) Higher magnification of black boxed regions in A, B and C show their respective lower incisors. Note the absence of a lower incisor in the *Sox2^{cKO}* mice (E). Lower incisors were observed in rescue mice (F). D', F') Higher magnification of the blue-boxed LaCL (D) shows cells in the stellate reticulum (stem cells) surrounded by the polarized outer and inner enamel epithelium in the control (D'). However, in the rescue mice a LaCL is formed but contains fewer progenitor cells and the outer and inner enamel epithelial cells are not well polarized (blue box, F'). D'', F'') Higher magnification of the green box in D and F. The rescue LIs (F'') show a lack of differentiation on the labial side and do not contain the differentiated odontoblasts, ameloblasts or stratum intermedium observed in the control incisors (D''). AM, ameloblast; OD, odontoblast; LaCL, labial cervical loop; SI, stratum intermedium; OEE, outer enamel epithelium; IEE, inner enamel epithelium; DL, dental lamina. Scale bars, 100µm.

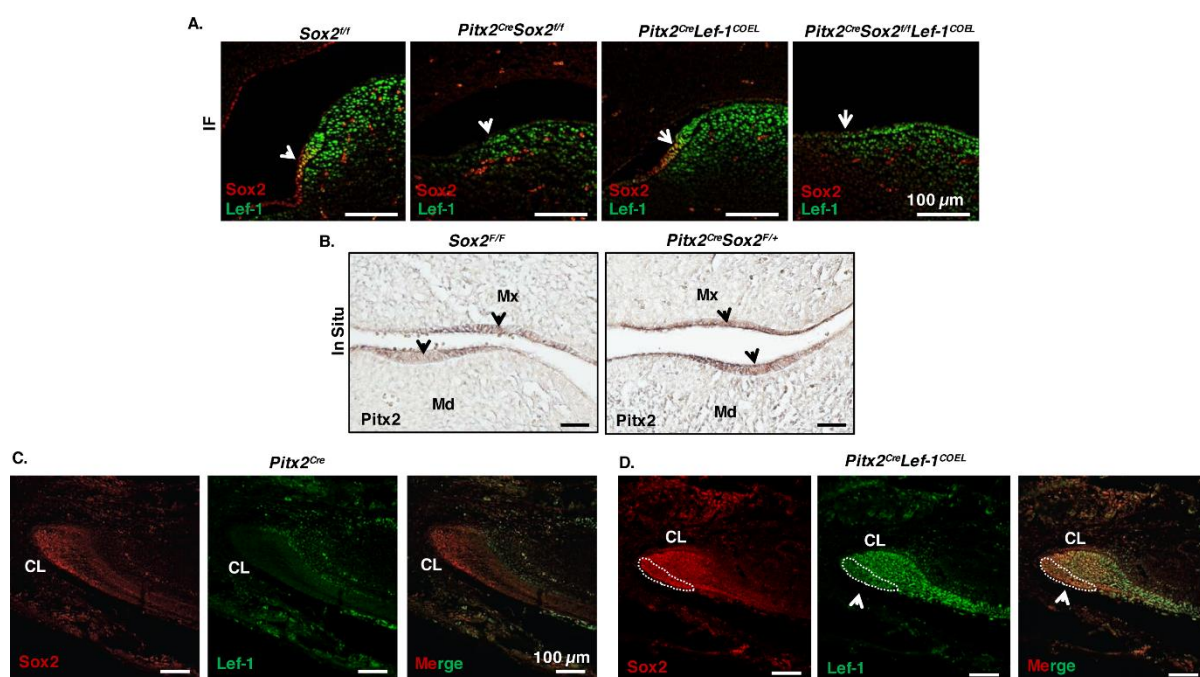


Figure S8. Sox2 and Lef-1 act independently to regulate early incisor development.

A) Merged photos of Sox2 and Lef-1 immunofluorescence staining in E11.5 *Sox2^{F/F}*, *Sox2^{KO}*, *COEL* and rescue embryos, showing the juxtaposed expression domains of these two factors. Loss of *Sox2* does not affect Lef-1 expression, and over expression of Lef-1 does not affect Sox2 expression. Arrows denote the dental placodes.

B) *Pitx2* in situ hybridization experiments showing *Pitx2* expression in the lower incisor placodes of E11.5 embryos. The arrows denote the incisor epithelial thickenings.

C, D) Sox2 and Lef-1 immunofluorescence staining in the LaCL of E18.5 *Pitx2^{Cre}* and *COEL* embryos, respectively. Lef-1 over expression (D) creates a new stem cell compartment (arrow). These cells express Sox2 but have reduced Lef-1 expression compared to Lef-1 expression in the other regions of the LaCL.

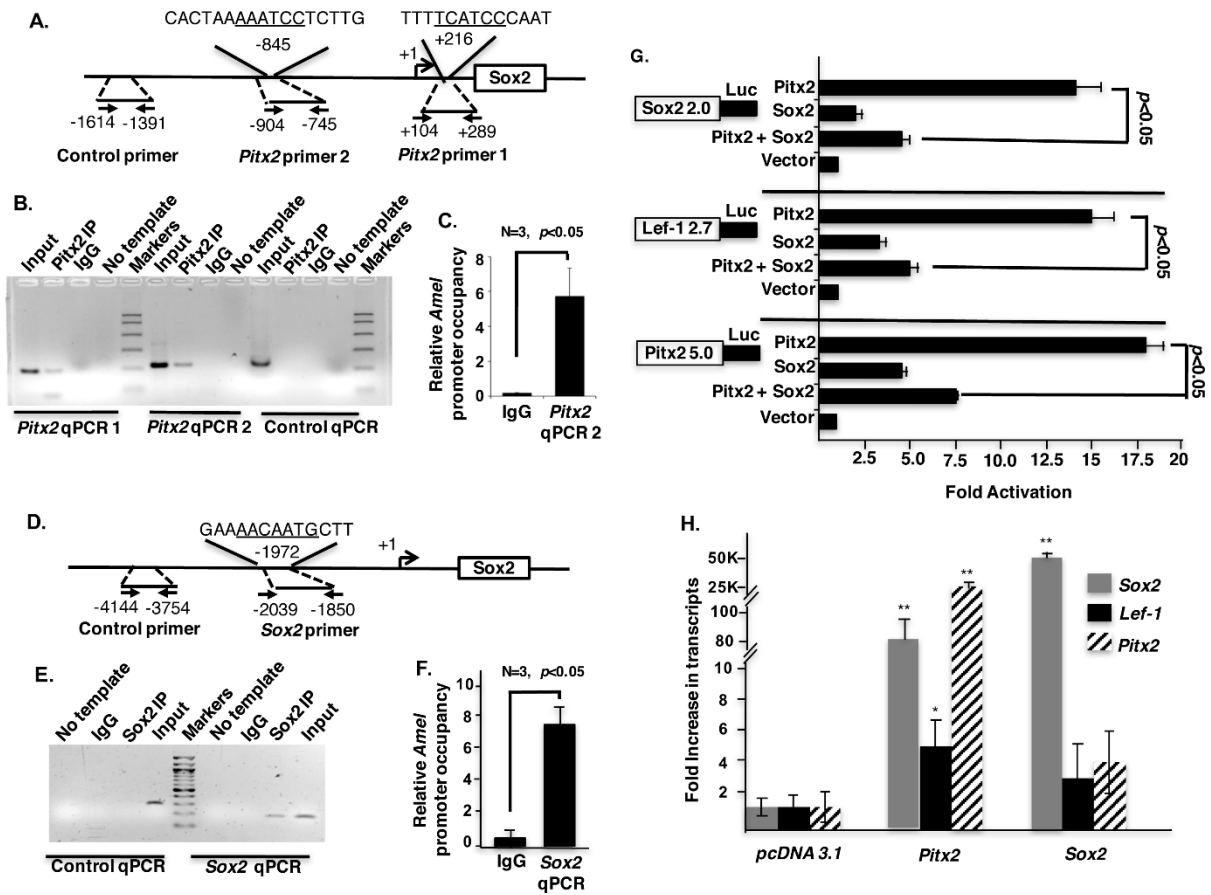


Figure S9. Endogenous Pitx2 and Sox2 bind to elements in the Sox2 promoter.

A) Schematic of the *Sox2* promoter region displaying two putative Pitx2 binding sites (216bp downstream of the transcriptional start site (TSS) and 845bp upstream of the TSS). The binding sequences are underlined. **B)** ChIP assays were performed on LS-8 cells and PCR products were resolved on agarose gels. Pitx2 antibody (Ab) immunoprecipitated (IP) the chromatin containing the Pitx2 binding sites but not a control site which did not contain a putative Pitx2 binding site. **C)** ChIP-qPCR analyses to assess the enrichment of the binding by Pitx2 Ab compared to IgG using Pitx2 primer 2 probes. **D)** A putative Sox2 binding site was identified at position 1972 upstream of *Sox2* TSS. Primers used to amplify the putative binding site and control site, which doesn't have a putative Sox2 binding, are indicated. **E)** ChIP assays were carried out on LS-8 cells by using a Sox2 Ab and the PCR results demonstrate that endogenous Sox2 binds to this Sox2 binding site in the Sox2 promoter region. **F)** ChIP-qPCR shows an 8-fold enrichment by using Sox2 Ab to pull-down this chromatin region compared to using IgG. **G)** Expression plasmids containing the Pitx2, Sox2, and vector-only cDNAs were co-transfected into LS-8 cells with a luciferase reporter plasmid whose expression was driven by the *Sox2*, *Lef-1* or *Pitx2* promoter. Luciferase activity is shown as mean-fold activation compared to activation in the presence of empty mock expression plasmid. All luciferase activities were normalized to β -galactosidase expression. **H)** *Sox2*, *Lef-1* and *Pitx2* transcripts from LS-8 cells transfected with vector only, Pitx2 or Sox2 were assessed by real-time PCR. The *Pitx2*, *Sox2* and *Lef-1* mRNA level in overexpressing Pitx2 and Sox2 cells were compared to overexpressing empty vector control cells. Pitx2 activates endogenous *Sox2* and *Lef-1* expression while overexpression of Sox2 shows no significant changes in endogenous expression levels of either *Lef-1* or *Pitx2* (N=3). All data normalized to β -actin transcripts. *, p<0.05. **, p<0.001. (Where are the * in panel H? please see the attached new fig S9)

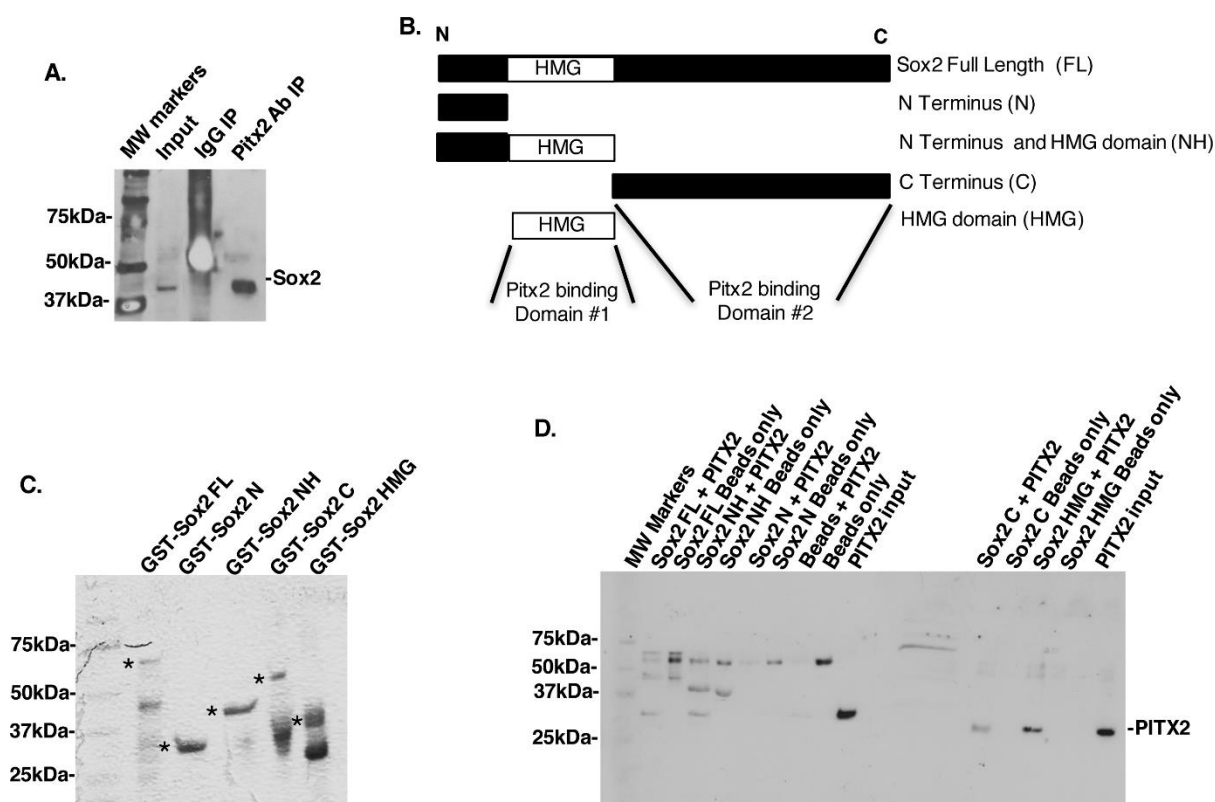


Figure S10. Sox2 interacts with Pitx2 through Sox2 HMG and C-terminal domains.

A) Immunoprecipitation (IP) of endogenous Sox2 using the Pitx2 Ab in LS-8 cells. The input was 5% of the lysate used in the IP assays. IgG used as a control did not IP the Sox2 protein, whereas the Pitx2 Ab did IP the Sox2 protein. **B)** Schematic of the GST-Sox2 truncated constructs used to determine the protein interaction domain of Sox2. The two Pitx2 binding domains are shown. **C)** GST-Sox2 constructs were bacteria expressed, purified and used in the GST-pull down assay. The fusion proteins are shown on a coomassie blue stained SDS PAGE gel. **D)** Purified Pitx2 protein was incubated with the GST-Sox2 constructs to determine which regions of Sox2 bound Pitx2. Pitx2 bound to the HMG and C-Terminal domains of Sox2.